1971

Analysis of continuous composite beams, Dec. 1971

Y. C. Wu.

R. G. Slutter

J. W. Fisher

LEHIGH UNIVERSITY

OFFICE
OF
RESEARCH

ANALYSIS OF CONTINUOUS COMPOSITE BEAMS

BY
YAO-CHING WU
R. G. SLUTTER
J. W. FISHER

FRITZ ENGINEERING LABORATORY REPORT NO. 359.5

ANALYSIS OF CONTINUOUS COMPOSITE BEAMS

by

Yao-Ching Wu

R. G. Slutter

J. W. Fisher

This research was conducted by

Fritz Engineering Laboratory

Lehigh University

for

Pennsylvania Department of Transportation

in cooperation with the

Federal Highway Administration

Fritz Engineering Laboratory
Department of Civil Engineering
Lehigh University
Bethlehem, Pa.

December 1971

Fritz Engineering Laboratory Report No. 359.5

TABLE OF CONTENTS

TABLE OF CONTENTS (continued)

LIST OF FIGURES

LIST OF FIGURES (continued)

ACKNOWLEDGMENTS

The experimental and theoretical studies summarized in this report were part of a research project on the development of design criteria for continuous composite steel and concrete bridges. This work was sponsored by the Pennsylvania Department of Transportation and the Federal Highway Administration. All of the work was conducted at Fritz Engineering Laboratory.

Th The writers wish to thank Dr. J. H. Daniels and Mr. I. Garcia for their aid in both the experimental and theoretical programs. The aid of the Fritz Engineering Laboratory Staff is gratefully acknowledged, especially Messrs. K. Harpel and H. Sutherland, for their help in the experimental program. The manuscript was typed by Mrs. Dorothy Fielding.

ABSTRACT

A method of analysis was developed for continuous composite beams with incomplete interaction. The method is general and can be used for any continuous composite beam system. The analysis may include the elastic and inelastic behavior of all elements of the continuous composite beam, as well as the effect of shrinkage and a prestressing force in the concrete slab.

The theoretical results were compared with the experimental results of laboratory tests on continuous beams. Satisfactory correlation was obtained between the analysis and the experimental values of slab force, shear connector loads and strain distribution in the cross-section.

The basic assumptions involved in the analysis are that the curvatures are the same for the slab and the beam and that the strain distribution in the slab and the beam are linear though not necessarily continuous across the interface. On the basis of these assumptions a set of simultaneous equations was derived from the equilibrium and the compatibility conditions with the unknowns as the axial force in the slab and the beam. A direct method of solving the equations with the aid of a computer was employed; this method was also extended to apply in the inelastic range. The method of analysis was made as general as possible so that a wide range of practical problems could be solved.

Recommendations for the number and spacing of shear connectors, and the amount and arrangement of the longitudinal reinforcing steel in the negative moment region of continuous composite bridges are made.

1. INTRODUCTION

1.1 General

Composite construction has been used with increasing frequency both in bridges and in buildings as a result of the 1944 AASHO Specification[1,2] and the simplified design provisions introduced by the 1961 AISC Specification.[3] Relatively little continuous composite construction has been employed in bridges due to a lack of comprehensive design provisions for such structures.

The behavior of a continuous composite beam in the negative moment region is quite different from that in the positive moment region. The concrete slab in the negative moment region is subjected to a tensile force and cracks, even under service loads. The flexibility of the concrete slab is not uniform over the negative moment region since the stiffness near cracks is less than the stiffness of the uncracked slab.

The behavior of the cracked slab can be described if the crack pattern, spacing and width were known. These can not be found directly by the application of elementary analysis. The behavior of the slab is also influenced by the load-slip relationship of the shear connectors. A limited investigation of this has been completed.[4]

With the increasing emphasis that will be placed on highway safety in the future, greater utilization of continuous composite beams is likely because of the desirability for increased span lengths, in order to eliminate the center piers of overpass structures.

Currently the AASHO Specification,[5] the AISC Specification,[6] and the British Code of Practice[7] cover methods of design for simple span members that consider both strength and performance. The provisions for the design of the negative moment region in continuous beams are not as fully developed as provisions for designing the positive moment region of composite members. For instance, in specifying the number of shear connectors in the negative moment region the AASHO Specification is based on the area of longitudinal reinforcement in the concrete slab whereas the British Code of Practice considers the entire concrete slab.

The participation of the concrete slab over the negative moment region has been examined in the past by two theories: (1) as a composite beam with complete interaction considering only the steel beam and reinforcement, and (2) as a tie bar with tension resisted by the continuous reinforcement anchored near the adjacent points of contraflexure. Neither of these theories adequately describes the behavior of the composite beam in the negative moment region and consequently the stresses in the longitudinal reinforcement and shear connectors can not be accurately determined. Some experimental studies of the behavior of the negative moment region of composite beams have been made.

There exists a need for a specific method of analysis in order to evaluate the actual stresses in the critical components and to include the effect of shrinkage. More detailed design specifications for continuous composite construction are also needed. There is also the need for the development of design criteria which will provide for satisfactory crack control in the concrete slab over the negative moment region and specification provisions to guard against fatigue failure of all elements in the negative moment region.

1.2 Previous Work

As early as the 1920's the composite steel and concrete beam was analyzed by the theories based on the transformed area method by assuming the complete interaction along the interface of the two elements. Practically all experimental studies have shown that the transformed area method could be applied to analyze the composite beams as long as the bond along the interface of the two elements was present. It was observed that the interaction along the interface of the composite beam with mechanical shear connectors was never complete. Nevertheless, the transformed area method could be used for simple beams, if the connectors were adequately designed. Later new theories were developed to account for the slip along the steel and concrete interface.

Stussi[8] developed a solution by allowing slip along the interface and assuming that (a) the load acting on the individual connector was directly proportional to the slip, (b) a discrete shear connection exists between the slab and the beam, (c) strain was linear in the slab and the beam, (d) the component elements deflected equally at the interface, and (e) horizontal forces acting on the slab or on the beam introduced by connectors act at the centroids of the slab and the beam cross-sections. The solution involved a system of linear equations based on the compatibility or continuity at the locations of the connectors as a function of the deformation of the concrete slab and beam between the connectors along the interface. The solution of the system of simultaneous equations gives the longitudinal forces acting on individual connectors.

Newmark[9] derived a differential equation for a composite beam of two different material elements. Instead of Stussi's assumption of a discrete shear connection, he assumed that the shear connection was continuous. The axial force acting on the slab or beam induced by flexure through the action of the shear connectors at the interface was an unknown of his differential equation.

Baldwin's solution[10] involved an expression for a relationship of connector force Q and the connector slip γ. With symmetry of loading, a simply supported composite beam has zero slip at midspan. By assuming a curvature and axial force in the concrete slab or beam at the section of the midspan, a resisting moment could be evaluated and compared with the external bending moment caused by the symmetrically applied loads. From the compatibility condition at the locations of the connectors relative to the deformation of the concrete slab and the beam between the connectors along the interface, the axial force at the next section was determined. Proceeding in this manner toward the support the axial force was compared with the boundary condition. If the boundary condition was not satisfied, the axial force at midspan was estimated again and solution was repreated until the boundary condition was satisfied.

Dai and others[11] followed Stussi's method very closely. A system of linear equations were developed from compatibility at the locations of connectors related to the deformation of the concrete slab and steel beam between the connectors along the interface. A non-linear relationship of the load-slip curve for connectors was used to modify the system of linear equations. The non-linear stress-strain relationship

of materials was also considered by a numerical procedure. Simply supported composite beams were analyzed both in the elastic and inelastic ranges.

Kaldjian[12] analyzed simply supported composite beams by a combination of two-dimensional isoparametric elements with two-dimensional linkage elements at the interface of composite or layered structural elements. He assumed that (a) each layer or composite element was connected to the next at specified points through the shear connectors, (b) the force in a shear connector was proportional to the slip of the connector at the interface, (c) no separation existed along the interface, and (d) friction forces along the interface were neglected. Two-dimensional linkage elments along the interface satisfy the first three assumptions. The linkage elements are made of two mutually perpendicular springs with spring constants K_H and K_V. Each spring can be assigned independently any value desired. Two-dimensional isoparametric finite elements with eight nodal points per element are known to yield very high accuracy with very few elements. Ten elements were employed in his analysis of three-layered beams with the desired accuracy of results. The element can be formed into the actual curved shapes, therefore, the boundaries between elements or external need not be straight. A load-slip relationship of a shear connector was expressed by a Ramberg-Osgood function. Because of the non-linearity of the shear connectors an increment procedure was employed until the full load was reached.

The ultimate strength theory of composite beams with a concrete slab and steel beam was based solely on the statical equilibrium of internal element forces. The advantage of this analysis lies in its simplicity. The development of the 1961 AISC Specification was based on studies

reported by Slutter and Driscoll.[13] If strain hardening was neglected and the yield criteria was not violated for any elements this represented a lower bound to the actual ultimate capacity of the composite beam.

1.3 Object and Scope

The purpose of this study was to develop a general numerical method of analysis for a continuous composite beam. The composite beam was considered to be a series of discrete slab and beam elements. A mathematical model was developed by replacing the continuous material of the composite beam by an equivalent system of lumped volumes which were connected at discrete points. A set of simultaneous equations with unknown forces acting at the centroids of the slab or the beam in each element was derived and also resulted in the same simultaneous equations as derived previously in the linear range of the elements.[12] A computer program was developed to carry out the numerical calculations in the analysis. The analysis and the method of solution has been made as general as possible in order to provide solutions of a wide variety of practical problems.

Suitable variables such as the number and spacing of shear connectors, the required amount of longitudinal reinforcing steel in the negative moment region, the effect of shrinkage and prestressing of the concrete slab in the continuous composite beams were examined. The results of four tests of two-span continuous composite beams conducted at Fritz Engineering Laboratory were compared with the theoretical results developed in this study.

2. THEORETICAL ANALYSIS

2.1 Composite Beam Analysis

A composite beam can be analyzed by considering it as a series of one dimensional elements. The axis of the composite beam can be taken along the interface of the concrete slab and steel beam. A finite number of nodal points can be assumed at the locations of shear connectors.

A system of nodal displacements, u_1, u_2, u_3, ... u_i, u_{i+1}... as illustrated in Fig.1a can be assumed to occur at the nodal points. The elongation of element i may be expressed in terms of the displacement at nodal point i+1 minus the displacement at nodal point i, that is $u_{i+1} - u_i$.

At nodal point i there are three linear forces to be considered: the connector force Q_i acting in the same direction as the displacement u_i, and the two boundary forces F_i and F_{i-1} as shown in Fig.1b. Forces F_i and F_{i-1} were considered to be positive when acting on nodal point (i) as illustrated in Fig. 2. The two elements (i) and (i-1) meet at nodal point i. Equilibrium requires that:

$$F_i - F_{i-1} = Q_i \tag{2.1}$$

Boundary conditions require that the element forces at the ends of a composite beam be zero.

If one considers the element (i), the elongation of the slab is given by $\int \epsilon_s \cdot ds$ and the beam by $\int \epsilon_b \cdot ds$. Slip in the element (i) can be expressed as $u_{i+1} - u_i$. Because the connectors i and i+1 are attached to the beam, the elongation of the slab relative to the beam can be expressed as $\int \epsilon_s \cdot ds - \int \epsilon_b \cdot ds$ or $\int (\epsilon_s - \epsilon_b) ds$. This must be equal to the slip that occurs in element (i), that is:

$$\int (\epsilon_s - \epsilon_b) \cdot ds = u_{i+1} - u_i \qquad (2.2)$$

The same assumptions that were employed in earlier elastic analyses by Stussi, Newmark and others[8,9,10,11,12] were also used for the elements. These are:

1. Curvatures of the slab and the beam were assumed to be the same.

2. The distribution of strain in the slab and the beam was assumed to be linear at all times but a discontinuity of the strain distribution was allowed at the interface, as shown in Fig. 2.

3. A non-linear stress-strain relationship for the slab and the beam, and a non-linear load-slip relationship for shear connectors were considered.

4. An initial strain caused by shrinkage of the concrete slab, prestressing the concrete slab, or differential expansion in the slab and beam can be accounted for.

If an initial strain ϵ_{sh} is taken into account, the elongation of the slab relative to the beam in element (i) becomes

$$\int(\epsilon_s - \epsilon_b)ds + \int\epsilon_{sh} \cdot ds = u_{i+1} - u_i \qquad (2.3)$$

Equation 2.3 considers deformation within the element relative to the nodal points at the ends of the element. Therefore, it is independent of the material properties which may be linear or non-linear. The unknown forces F_i acting in element (i) are asumed to act at the centroid of the slab and the beam as shown in Fig. 3. C_s and C_b are the distances from the centroids of the slab and the beam to the interface. M_s and M_b are the bending moments generated in the slab and the beam. The unknown forces F_i are transmitted by shear connectors at discretely distributed nodal points. The force F_i is maximum when the shear connectors are infinitely stiff and zero when no connectors are provided. Mechanical shear connectors provide a finite stiffness. Since the sum of the three resisting bending moments $F\ (C_s + C_b)$, M_s and M_b in the element (i) must equal the external moment acting on the element a reduction in the force F_i due to incomplete interaction or finite stiffness of the shear connectors will lead to an increase in the moments M_s and M_b.

2.2 Evaluation of Element Properties

Once the force-displacement relationships for individual elements are known, it is possible to evaluate an assembled structure.

The forces or stress resultants acting on the slab of the element (i) are F and M_s. Because the axis of the composite beam was taken along the interface of the concrete slab and the steel beam, the force-displacement relationships were evaluated along the interface. The stress in the slab along the interface can be expressed as:

$$\sigma_s = \frac{F}{A_s} - \frac{M_s \cdot C_s}{I_s} \tag{2.4}$$

Where A_s and I_s are cross-sectional area and moment of inertia of the slab.

If the stress-strain relationship is linear for the element (i), the strain ϵ_s at the slab interface will be

$$\epsilon_s = \frac{1}{E_s}\sigma_s = \frac{1}{E_s}\left(\frac{F}{A_s} - \frac{M_s \cdot C_s}{I_s}\right) \tag{2.5}$$

The stress and strain in the steel beam at the interface can be expressed as

$$\sigma_b = -\frac{F}{A_b} + \frac{M_b \cdot C_b}{I_b} \tag{2.6}$$

$$\epsilon_b = \frac{1}{E_b}\left(-\frac{F}{A_b} + \frac{M_b \cdot C_b}{I_b}\right) \tag{2.7}$$

Where A_b, I_b and E_b are area, moment of inertia, and modulus of elasticity of the steel beam.

The elongation of the slab relative to the beam can be expressed in terms of forces or stress resultants.

$$\int(\epsilon_s - \epsilon_b) \cdot ds = \int[\frac{1}{E_s}(\frac{F}{A_s} - \frac{M_s \cdot C_s}{I_s}) - \frac{1}{E_b}(-\frac{F}{A_b} + \frac{M_b \cdot C_b}{I_b})] \cdot ds$$

$$= \int[(\frac{F}{E_s A_s} + \frac{F}{E_b A_b}) - (\frac{M_s \cdot C_s}{E_s \cdot I_s} + \frac{M_b \cdot C_b}{E_b \cdot I_b})]\, ds \tag{2.8}$$

Integration is taken over the entire length of the element (i). There are three unknown forces, F, M_s, and M_b in Eq. (2.8). It is possible to eliminate the two unknown forces M_s and M_b using the assumption of equal curvature and equilibrium of element (i).

The curvature of the slab and the beam are the same

$$\phi_s = \phi_b \tag{2.9}$$

For a linear stress-strain relationship, curvature is proportional to the bending moment.

$$\phi_s = \frac{M_s}{E_s I_s} \tag{2.10}$$

$$\phi_b = \frac{M_b}{E_b I_b} \tag{2.11}$$

$$\frac{M_s}{E_s I_s} = \frac{M_b}{E_b I_b} = \frac{M_s + M_b}{E_s I_s + E_b I_b} \tag{2.12}$$

Moment equilibrium requires that

$$F \cdot Z + M_s + M_b = M \tag{2.13}$$

$$M_s + M_b = M - F \cdot Z \tag{2.14}$$

where

$$Z = C_s + C_b \tag{2.15}$$

By eliminating M_s and M_b this yields

$$\int(\epsilon_s-\epsilon_b)ds=\int[(\frac{F}{E_sA_s}+\frac{F}{E_bA_b})-(\frac{M-FZ}{E_sI_s+E_bI_b}\cdot C_s+\frac{M-FZ}{E_sI_s+E_bI_b}\cdot C_b)]\cdot ds$$

$$=\int[(\frac{F}{E_sA_s}+\frac{F}{E_bA_b})-(\frac{M-FZ}{E_sI_s+E_bI_b}Z)]\cdot ds \tag{2.16}$$

If F is the average force in element (i) and Δs is the length of element (i),

$$\int(\epsilon_s-\epsilon_b)ds=(\frac{1}{E_sA_s}+\frac{1}{E_bA_b}+\frac{Z^2}{E_sI_s+E_bI_b})F\cdot\Delta s-\frac{MZ}{E_sI_s+E_bI_b}\cdot\Delta s \tag{2.17}$$

2.3 Connector Force and Nodal Displacement Relationship

The force Q_i acting on connector i at nodal point i can be expressed in terms of nodal displacement u_i. If a linear relationship exists for the load-slip curve,

$$Q_i = k_i u_i \tag{2.18}$$

where k_i is the slope of the load-slip curve at nodal point i.

For a non-linear relationship the force Q_i may be expressed as a function of u_i

$$Q_i = f(u_i) \tag{2.19}$$

The value of K_i at a point (u_i, Q_i) can be expressed in terms of the first derivative of Q_i with respect to u_i.

$$K_i = f'(u_i) = \frac{d\ Q_i}{d\ u_i} \tag{2.20}$$

If the load-slip relationship is linear, the slip of element (i) may be expressed in terms of the nodal displacements at point i and i + 1. When expressed in terms of the connector forces and the stiffness of the load-slip curve this yields

$$u_{i+1} - u_i = \frac{Q_{i+1}}{K_{i+1}} - \frac{Q_i}{K_i} \tag{2.21}$$

If the connector forces are expressed in terms of the forces F_i this yields

$$u_{i+1} - u_i = \frac{F_{i+1} - F_i}{K_{i+1}} - \frac{F_i - F_{i-1}}{K_i}$$

$$= \frac{F_{i+1}}{K_{i+1}} - \left(\frac{1}{K_{i+1}} + \frac{1}{K_i}\right) F_i + \frac{F_{i-1}}{K_i} \tag{2.22}$$

When the load-slip curve is non-linear, the slip of element (i) may be reduced to a linear relationship of the load-slip curve for connectors as follows. A tangent can be constructed at any point on the load-slip curve shown in Fig. 4(a). This tangent intersects the horizontal axis at A.

Let $\overline{OA} = d_i$ (a)

From geometry, the displacement u_i can be determined as

$$\overline{CA} = \frac{Q_i}{K_i} \qquad (b)$$

$$\overline{CO} = u_i \qquad (c)$$

$$\overline{CA} = \overline{OA} + \overline{CO} = d_i + u_i \qquad (d)$$

$$u_i = \frac{Q_i}{K_i} - d_i \qquad (e)$$

Therefore the slip in element (i) which equals the relative displacement of nodal points i + 1 and i can be expressed as

$$u_{i+1} - u_i = \left(\frac{Q_{i+1}}{K_{i+1}} - d_{i+1}\right) - \left(\frac{Q_i}{K_i} - d_i\right)$$

$$= \frac{1}{K_{i+1}} F_{i+1} - \left(\frac{1}{K_{i+1}} + \frac{1}{K_i}\right) F_i + \frac{1}{K_i} F_{i-1} - (d_{i+1} - d_i)$$

(2.23)

The only difference between a linear and a non-linear relationship is the term $(d_{i+1} - d_i)$ which must be subtracted from the slip of element (i) or the relative displacement of nodal points i + 1 and i.

If the load-slip relationship is convex as illustrated in Fig. 4(a), the displacement u_i can be expressed as

$$\overline{CA} = \overline{OA} + \overline{CO} \qquad (f)$$

$$= - \overline{AO} + \overline{CO} \qquad (g)$$

$$\overline{CA} = - d_i + u_i \qquad (h)$$

$$u_i = \frac{Q_i}{K_i} + d_i \qquad (i)$$

The slip of the element (i) can be expressed as

$$u_{i+1} - u_i = \left(\frac{Q_{i+1}}{K_{i+1}} + d_{i+1}\right) - \left(\frac{Q_i}{K_i} + d_i\right)$$

$$= \frac{1}{K_{i+1}} F_{i+1} - \left(\frac{1}{K_{i+1}} + \frac{1}{K_i}\right) F_i + \frac{1}{K_i} F_{i-1} + (d_{i+1} - d_i)$$

(2.24)

The term $(d_{i+1} - d_i)$ is now added to the slip of the element (i) when the load-slip curve is concave upward as shown in Fig. 4(b).

2.4 Basic Equations

The compatibility equation which relates the elongation in the slab relative to the beam in element (i) to a differential displacement at nodal points i+1 and i at the ends of element (i) can be expressed in terms of the unknown forces F_i. For a linear load-slip relationship this yields

$$\frac{F_{i-1}}{K_i} - \left(\frac{1}{K_i} + \frac{1}{K_{i+1}}\right) F_i + \frac{F_{i+1}}{K_{i+1}} = \left(\frac{1}{E_s A_s} + \frac{1}{E_b A_b} + \frac{Z^2}{E_s I_s + E_b I_b}\right) F_i \cdot \Delta s$$

$$- \frac{M Z}{E_s I_s + E_b I_b} \Delta s + \int \epsilon_{sh} \cdot ds$$

(2.25)

The unknown forces F_{i-1}, F_i, and F_{i+1} are evaluated in element (i) and the two adjacent elements (i - 1) and (i + 1). All terms on the right side of Eq. (2.25) are determined from element (i). In the

absence of initial strains in the slab the term $\int \epsilon_{sh} \cdot ds$ does not exist. When

$$\alpha_i = \frac{1}{E_s A_s} + \frac{1}{E_b A_b} + \frac{Z^2}{E_s I_s + E_b I_b} \tag{2.26}$$

$$\beta_i = \frac{Z}{E_s I_s + E_b I_b} \tag{2.27}$$

Equation (2.25) can be expressed as

$$\frac{1}{K_i} F_{i-1} - \left(\frac{1}{K_i} + \frac{1}{K_{i+1}} + \alpha_i \Delta s\right) F_i + \frac{1}{K_{i+1}} F_{i+1} = - M_i \beta_i \Delta s_i + \int_{\Delta s_i} \cdot \epsilon_{sh} \cdot ds \tag{2.28}$$

For i = k, 2, 3, ... n Eq. (2.28) leads to

$$\frac{1}{K_1} F_o - \left(\frac{1}{K_1} + \frac{1}{K_2} + \alpha_1 \Delta s_1\right) F_1 + \frac{1}{K_2} F_2 = - M_1 \beta_1 \Delta s_1 + \int_{\Delta s_1} \epsilon_{sh} \cdot ds$$

$$\frac{1}{K_2} F_1 - \left(\frac{1}{K_2} + \frac{1}{K_3} + \alpha_2 \Delta s_2\right) F_2 + \frac{1}{K_3} F_3 = - M_2 \beta_2 \Delta s_2 + \int_{\Delta s_2} \epsilon_{sh} \cdot ds \tag{2.29}$$

$$\frac{1}{K_3} F_2 - \left(\frac{1}{K_3} + \frac{1}{K_4} + \alpha_3 \Delta s_3\right) F_3 + \frac{1}{K_4} F_4 = - M_3 \beta_3 \Delta s_3 + \int_{\Delta s_3} \epsilon_{sh} \cdot ds$$

. . . . .
. . . . .

$$\frac{1}{K_n} F_{n-1} - \left(\frac{1}{K_n} + \frac{1}{K_{n+1}} + \alpha_n \Delta s_n\right) F_n + \frac{1}{K_{n+1}} F_{n+1} = - M_n \beta_n \Delta s_n + \int_{\Delta s_n} \epsilon_{sh} \cdot ds$$

There are n equations and n + 2 unknown forces F_0, F_1, F_2 ... F_n and F_{n+1}. At the ends of a composite beam boundary conditions require $F_0 = 0$ and $F_{n+1} = 0$. Therefore the unknown forces F_1, F_2, ... F_n can be determined from n equations.

2.5 Modification of Newmark's Differential Equation

It is interesting to compare Eqs. (2.28) with Newmark's differential equation[9]. Newmark's differential equation may be written as:

$$\frac{d^2 F}{dx^2} - F \left(\frac{K}{S} \frac{\overline{EI}}{\Sigma EI \; \overline{EA}}\right) = - \frac{K}{S} \frac{MZ}{\Sigma EI} \tag{2.30}$$

In the derivation it was assumed that the shear connection is continuous along the interface of the slab and the beam, therefore the ratio of K divided by S is constant. In this study K is considered as a variable and the differential equation was changed into a set of simultaneous equations by using a finite difference method. Equation (2.30) can be written as

$$\frac{S}{K} \frac{d^2 F}{dx^2} - F \frac{\overline{EI}}{\Sigma EI \; \overline{EA}} = - \frac{MZ}{\Sigma EI} \tag{2.31}$$

If the stiffness of connectors is K_i and the distance between connectors is Δs, as shown in Fig. 5, the first term of the differential equation may be written as

$$\frac{s}{K}\frac{d^2F}{dx^2} = s\frac{d}{dx}\left(\frac{1}{K}\frac{dF}{dx}\right) = \Delta s\frac{1}{\Delta x}\left[\frac{1}{}\left(\frac{F_{i+1} - F_i}{K_{i+1}} - \frac{F_i - F_{i-1}}{K_i}\right)\right]$$

$$= \frac{1}{\Delta s_i}\left[\frac{F_{i+1}}{K_{i+1}} - \left(\frac{1}{K_{i+1}} + \frac{1}{K_i}\right)F_i + \frac{F_{i-1}}{K_i}\right] \qquad (2.32)$$

where $\Delta s = \Delta x = s$.

The unknown force F_i is evaluated at the center of the element (i) between connectors i and i + 1.

The second term of the differential equation may be written as

$$F\frac{\overline{EI}}{\Sigma EI\ \overline{EA}} = F\left(\frac{1}{E_sA_s} + \frac{1}{E_bA_b} + \frac{Z^2}{E_sI_s + E_bI_b}\right) = F_i\ \alpha_i \qquad (2.33)$$

The right hand term of the differential equation may be written as

$$-\frac{MZ}{\Sigma EI} = -\frac{MZ}{E_sI_s + E_bI_b} = -M_i\ \beta_i \qquad (2.34)$$

Combining all terms of the differential equation leads to a set of simultaneous equations, thus:

$$\frac{F_{i-1}}{K_i} - \left(\frac{1}{K_i} + \frac{1}{K_{i+1}} + \alpha_1\ \Delta s_i\right)F_i + \frac{F_{i+1}}{F_{i+1}} = -M_i\ \beta_i\ \Delta s_i \qquad (2.35)$$

These equations are the same as Eq. (2.28) except that the initial strains are not considered. The only difference between Newmark's differential equation and Eq. (2.28) is that the connector stiffness K_i is no longer constant.

2.6 Deflection, Strain Distribution, and Slip

The deflection along a composite beam may be approximated from the curvature of the slab ϕ_s or the beam ϕ_b. Hence,

$$\frac{d^2 y}{dx^2} = \frac{M_s}{E_s I_s} = \frac{M_b}{E_b I_b} = \frac{M - F Z}{E_s I_s + E_b I_b} \tag{2.36}$$

When expressed in finite difference form, this yields

$$y_{i-1} - 2y_i + y_{i+1} = \frac{M - F Z}{E_s I_s + E_b I_b} \Delta x^2 \tag{2.37}$$

Equation (2.37) results in a series of simultaneous equations

$$\begin{aligned}
y_o - 2y_1 + y_2 &= \frac{M_1 - F_1 Z_1}{E_{s1} I_{s1} + E_{b1} I_{b1}} \cdot \Delta x_1^2 \\
y_1 - 2y_2 + y_3 &= \frac{M_2 - F_2 Z_2}{E_{s2} I_{s2} + E_{b2} I_{b2}} \cdot \Delta x_2^2 \\
y_2 - 3y_3 + y_4 &= \frac{M_3 - F_3 Z_3}{E_{s3} I_{s3} + E_{b3} I_{b3}} \cdot \Delta x_3^3 \\
&\cdots \\
&\cdots \\
y_{n-1} - 2y_n + y_{n+1} &= \frac{M_n - F_n Z_n}{E_{sn} I_{sn} + E_{bn} I_{bn}} \cdot \Delta x_n^2
\end{aligned} \tag{2.38}$$

There are n equations and n unknown deflections since the boundary conditions provide two known deflections.

After finding the unknown forces F_i, the moment in the slab M_s and beam M_b may be obtained from Eq. (2.36)

$$M_s = E\ I\ \frac{M - F\ Z}{E_s I_s + E_b I_b} \tag{2.39}$$

$$M_b = E_b I_b\ \frac{M - F\ Z}{E_s I_s + E_b I_b} \tag{2.40}$$

When the stress-strain relationship is linear for the concrete slab or the steel beam, the strains in the top and bottom of these elements are given by

$$\epsilon_{sb} = \frac{1}{E_s}\left(\frac{F}{A_s} - \frac{M_s \cdot C_s}{I_s}\right) \tag{2.41}$$

$$\epsilon_{st} = \frac{1}{E_s}\left(\frac{F}{A_s} + \frac{M_s \cdot C_s}{I_s}\right) \tag{2.42}$$

$$\epsilon_{bb} = \frac{1}{E_b}\left(-\frac{F}{A_b} - \frac{M_b \cdot C_b}{I_b}\right) \tag{2.43}$$

$$\epsilon_{bt} = \frac{1}{E_b}\left(-\frac{F}{A_b} + \frac{M_b \cdot C_b}{I_b}\right) \tag{2.44}$$

After finding the unknown forces F_i for every element (i), the forces Q_i may be obtained from Eq.(2.1). The slip can be determined from the load-slip relationship.

Equation (2.29) may be expressed in matrix form and solved by elimination methods for the unknown slab forces F_o, F_1, F_2, ... F_n. The Gauss elimination method was used for this investigation. References pertaining to the development of the computer program and sources for the load-slip relationships are given in Appendix B.

3. INELASTIC ANALYSIS OF COMPOSITE BEAMS

3.1 General

Matrix structural analysis is a linear analysis procedure which is based on the principle of superposition. However, through the use of iterative or load increment procedure it is possible to extend the analysis into the non-linear range.

Non-linearity may be introduced into a composite beam in two ways, (1) the element stiffness may vary with the deformation of the element, and (2) the geometric configuration of the structure as a whole or elements themselves may change sufficiently under loading so that the equilibrium relationships of the structure are influenced. The second type of non-linearity involves the large displacement theory of the structure. Only the first type of non-linearity is considered in this study.

The properties of the element material usually have a general characteristic which uniquely defines the state of stress by the state of strain provided that a monotonic increase of the stresses or certain stress invariants occur.

The incremental load procedure was used to provide solutions to non-linear problems. The procedure gives a picture of the development of the plastic process or a history of the plastic process during load increments.

3.2 Incemental Load Analysis

It was assumed that the element material will become plastic when the strain exceeds a certain critical value. The top fiber strain in a concrete slab becomes non-linear when the elastic limit of the stress-strain relationship is exceeded. Stress beyond this limit is associated with a lower modulus. Different stress-strain relationships may be assigned to each element depending on the properties of the material which make up the element. The incremental analysis assumes that the load is applied in small increments. The unknown forces F_i acting on the concrete slab or the steel beam and the deflection are determined for each increment of load using the elastic analysis with modified stiffness.

The inelastic analysis was undertaken using the following procedure. A linear analysis can be used when the load-deformation relationship is linear between points 0 and 1 in Fig. 6. At point 1 the stress-strain relationship becomes non-linear. This means that the tangent to the stress-strain curve and the tangent modulus of the material (hereafter called the modulus) changes as the load and strain is increased.

At point 2 on the non-linear curve it is possible to construct a straight line $\overline{12}$ between points 1 and 2 and the modulus between points 1 and 2 is assumed constant (E'_{12} = constant), therefore E'_{12} is an average value of the actual stress-strain curve $\overset{\frown}{12}$ between points 1 and 2. The modulus is maximum at point 1 and

decreases along segment 12 of the curve to a minimum value at point 2. If the modulus along segment 12 of the curve is assumed constant, then proceeding from point 1 to point 2 is exactly the same as proceeding from point 0 to point 1 if the reference point has been changed from point 0 to point 1. Strains determined from Eqs. (2.5) and (2.7) are incremental strains that correspond to the increment of load.

After the application of each increment of load the average strains, stresses and moduli for both slab and steel beam are determined for each element. These values are used as initial values for the next load increment.

In this study when the top fiber strain exceeded a limiting value the concrete slab was divided into 10 slices. The strain in each slice and the corresponding stress was calculated. The average strain and stress for each load increment was determined for the concrete slab and the corresponding average modulus estimated as shown in Fig. 7. When the bottom fiber strain in the steel beam exceeded the yield strain the steel beam was divided into 42 slices. It will be more accurate if the flanges of the steel beam are divided into smaller slices than the web because the width of the flanges is much greater than that of the web. The average strain, stress, and modulus for each load increment were calculated as shown in Fig. 8. Different stress-strain relationships can be assigned to each slice if desired.

3.3 The Non-Linear Load-Slip Curve

The non-linear load-slip relationship for connectors can also be treated using an incremental load. A non-linear relationship for connectors can be assumed as $Q = f(u)$ as shown in Fig. 9. At point 1 a new origin is selected with the same non-linear relationship of load-slip for connectors but a different mathematical expression for the curve. The new function of the curve is $Q_i = f_1 (u_1)$. With the origin at 1 and $Q_1 = f_1 (u_1)$ the procedure is repeated. The connector forces and slips are determined by superimposing the results obtained for each load increment.

3.4 Ultimate Strength of Connectors

When a connector reaches its ultimate strength, the slope of the load-slip curve becomes 0, that is,

$$\frac{d\,Q}{d\,u_i} = K_i = 0 \qquad (3.1)$$

Equation (2.29) is not defined, because $K_i = 0$ and $1/K_i = \infty$. It is not possible to find the unknown forces F_i acting on the slab or on the steel beam. This difficulty can be overcome by combining adjacent elements with the connector at ultimate load.

When a connector at nodal point i is at ultimate the connector load Q_i is equal to Q_u. Because u_i is not defined the two adjacent elements (i - 1) and (i) can be combined with u_i as follows:

$$u_{i+1} - u_i = \left(\frac{Q_{i+1}}{K_{i+1}} - d_{i+1}\right) - \left(\frac{Q_i}{K_i} - d_i\right) \tag{3.2}$$

$$u_i - u_{i-1} = \left(\frac{Q_i}{K_i} - d_i\right) - \left(\frac{Q_{i-1}}{K_{i-1}} - d_{i-1}\right) \tag{3.3}$$

by adding Eqs. (3.2) and (3.3)

$$u_{i+1} = u_{i-1} = \left(\frac{Q_{i+1}}{K_{i+1}} - d_{i+1}\right) - \left(\frac{Q_{i-1}}{K_{i-1}} - d_{i-1}\right) \tag{3.4}$$

The equilibrium conditions at nodal points i+1, i, and i-1 are defined by

$$F_{i+1} - F_i = Q_{i+1} \tag{3.5}$$

$$F_i - F_{i-1} = Q_i \tag{3.6}$$

$$F_{i-1} - F_{1-2} = Q_{i-1} \tag{3.7}$$

Because the connector at nodal point i is at ultimate, Eq. (3.6) can be expressed as

$$F_i - F_{i-1} = Q_u \tag{3.8}$$

Substituting Eqs. (3.5), (3.7), and (3.8) into Eq. (3.4) results in

$$\begin{aligned} u_{i+1} - u_{i-1} &= \frac{F_{i+1} - F_i}{K_{i+1}} - \frac{F_{i-1} - F_{i-2}}{K_{i-1}} - (d_{i+1} - d_{i-1}) \\ &= \frac{F_{i+1} - W_u - F_{i-1}}{K_{i+1}} - \frac{F_{i-1} - F_{i-2}}{K_{i-1}} - (d_{i+1} - d_{i-1}) \\ &= \frac{1}{K_{i+1}} F_{i+1} - \left(\frac{1}{K_{i+1}} + \frac{1}{K_{i-1}}\right) F_{i-1} \\ &\quad + \frac{1}{K_{i-1}} F_{1-2} - \frac{1}{K_{i+1}} - (d_{i+1} - d_{i-1}) \end{aligned} \tag{3.9}$$

3.5 Fracture of Connectors

When a connector reaches its ultimate displacement and finally fractures, the loading acting on the connector at the nodal point i becomes zero, that is $Q_i = 0$. Therefore,

$$F_i = F_{i-1} \tag{3.10}$$

Equation (3.9) reduces to

$$u_{i+1} - u_{i-1} = \frac{1}{K_{i+1}} F_{i+1} - \left(\frac{1}{K_{i+1}} + \frac{1}{K_{i-1}}\right) F_{i-1} + \frac{1}{K_{i-1}} F_{1-2} - (d_{i+1} - d_{i-1}) \tag{3.11}$$

The analysis described in this chapter is used in Chapter 5 to predict the behavior of several continuous composite beams.

4. SHRINKAGE

4.1 General

Shrinkage plays an important part in the behavior of continuous composite beams. In the negative moment regions of continuous composite beams tension develops in the steel bars at a crack because shear connectors prevent shortening of the concrete slab. More tension develops in the steel bars as live load is added.

For many years it has been accepted that the steel bars in the concrete slab control shrinkage cracking. Shrinkage of a concrete slab causes compressive stress in the steel bars and tensile stress in the concrete slab. The magnitude of the stresses developed in the steel bars and the concrete slab is dependent on the unit shrinkage strain of the concrete, tensile strength of the concrete slab, modulus of elasticity of the concrete, and the amount and size of the steel bars.

4.2 Mechanism of Crack Formation

The mechanism of crack formation based on Woolley's[14] analysis is that major stresses in the concrete slab are carried by the concrete until it cracks and then the steel bars carry the total stress at the crack. When the concrete slab is restrained at both

ends, the steel bar stress is transferred into the concrete slab by the bond between the steel bars and the concrete near the crack.

As shrinkage continues to take place the steel bar stress at the crack continues to increase. As the crack opens higher stresses occur in the surrounding concrete and other cracks form. The additional cracks will relieve the stress in the concrete slab and this process continues until the entire concrete slab has a system of small cracks equally spaced. In a bridge deck the crack spacing normally becomes the spacing of the transverse bars. When the amount of steel is inadequate to control the crack opening, excessive deformation occurs at cracks resulting in plastic deformation of the steel bars. The cumulative effect of the plastic deformation from shrinkage with cyclic loading produced by live loads on the structure can lead to a reduced fatigue life of the longitudinal bars.

4.3 Criteria

In a continuously reinforced concrete pavement, the pavement is restrained by friction of the subgrade. Whereas in any composite beam the concrete slab is restrained by shear connectors. Therefore, the two problems are similar with regard to the effect of shrinkage although the thermal stress situation may be different. On the basis of the crack formation pattern recommendations have been made for the percentage of steel area desired in continuously reinforced concrete pavement.[15] In a similar manner it is necessary to consider

a similar requirement for composite bridge decks since the minimum amount of longitudinal steel required for bridge slabs might exceed the distribution steel requirement in the current specification. The tensile strength of the concrete is the basis for selection of the amount of steel. In bridge slabs the amount of steel must be larger than in pavements because the tensile strength of the concrete in bridges is generally higher than that for pavements.

For a continuous composite beam the tensile yield strength of the longitudinal steel bars in the slab should be larger than the tensile capacity of the concrete slab particularly in the negative moment region[16,17]. When the tensile yield strength of the longitudinal steel bars is greater than that of the concrete slab in tension, additional cracks always form in the concrete slab due to combined shrinkage and tensile loading. On the other hand, when the tensile capacity of the slab is greater than the yield strength of the longitudinal steel bars, the steel bar continues to elongate at the crack instead of forming additional cracks in the slab.

4.4 Shrinkage Effect on Continuous Beams

The shrinkage effect is an important factor in the negative moment regions of continuous composite beams. Because shrinkage produces a sizable dimensional change in the concrete slab which is connected to the steel beam by mechanical shear connectors, deformation is induced into the steel beam producing forces on the shear connectors, concrete slab and steel beam, and a downward deflection

for a simple beam. For a simply supported member the shrinkage effect may be insignificant but for a continuous composite beam the shrinkage effect may be pronounced.

If the end connectors are very stiff the force induced by shrinkage will be resisted by the end connectors. In practice most connectors are flexible and the forces are distributed. The slope of the slab force distribution curve due to shrinkage near the ends of the composite beam is dependent on the load-slip relationships of the shear connectors.

When the shrinkage effect of a single span composite beam is analyzed, it is possible to extend the analysis to a continuous composite beam; since the deflection at the interior support of the two-span continuous beam is zero whereas the deflection at the midspan of a single span beam is not restricted to any value.

When shrinkage takes place the slab of the composite beam is shortened and shrinkage causes the beam to deflect downward. An upward restoring force must be applied at the location of any interior support. The magnitude of the concentrated load should be such that it would deflect the beam upward with the same magnitude of deflection as that due to shrinkage. The two values are superimposed and the deflection at the interior support was checked by the results of combining the two values.

The slab force induced by shrinkage can be analyzed easily in this study. It is merely necessary to specify the value of the

unit shrinkage strain for the initial strain ϵ_{sh} in the right side of the compatibility Eq. (2.29). When the shrinkage effect is considered separately from the effect of the externally applied loads, the value of M_i at the right side of Eq. (2.29) is zero.

There are some methods to minimize the effect of shrinkage in composite beams especially in the negative moment region. These are: (a) inducing a compressive force into the concrete slab over the negative moment region by means of prestressing the concrete slab, (b) jacking of the interior support, (c) casting the slab in shorter lengths in a checker board pattern. Jacking of the interior support does not produce permanent prestress in the slab, but it is an effective means of counteracting the effect of shrinkage without resorting to the high cost of prestressing.

The important variables influencing the amount of shrinkage are (1) concrete age, (2) curing conditions, (3) cross-section of member, (4) amount of reinforcement in the concrete slab, (5) shear connector stiffness, and (6) sequence of casting the slab. Only the effect of the latter three variables are of concern in this study.

4.5 Shrinkage Effect on Beam CC-4F

As an example of the effect of shrinkage on the behavior of a continuous member the slab force produced by shrinkage in beam CC-4F was considered[16]. The composite beam CC-4F was 50 ft.-10 in. long with two equal spans of 25 ft.-0 in. between supports. The beam consisted of a reinforced concrete slab 60 inches wide and 6 inches thick

interconnected to a W21x62 steel beam by 3/4 inch stud shear connectors 4 inches high. The rolled beam was fabricated drom ASTM A36 steel. Details of the continuous composite beam are shown in Figs. 10 through 12.

The full length of the continuous composite beam CC-4F was divided into 125 elements. All elements were interconnected at nodal points located at stud connectors except for a part of the negative moment region where connectors were omitted. Imaginary connectors were provided in the region where connectors were omitted in order to simulate friction between the concrete slab and the steel beam in this region. The slab was assumed to be cracked at intervals of 6 inches to simulate the actual crack pattern. The uncracked slab was also examined by mathematical models. As a result of the symmetry of the member, the 125 simultaneous equations were reduced to 63 equations for the mathematical model of the slab. The stress-strain relationships for the concrete slab and steel beam, and the load-slip relationships for each connector were first defined.

Figure 13 shows the force induced in the concrete slab due to the effect of shrinkage. Two different unit shrinkage strains of the concrete slab were examined. The lower value of 0.0002 is suggested by the AASHO Specifications[5]. The higher value was included to obtain an upper bound of the slab force. Figure 13 represents a single span composite beam due to unit shrinkage strains of 0.0002 and 0.0003.

Figure 14 shows the force induced in the concrete slab from shrinkage for the continuous composite beam of CC-4F. The effect of the interior support for the continuous composite beam CC-4F has been included in Fig. 14. The two curves correspond to shrinkage strains of 0.002 and 0.003 respectively. These two values are obtained by combining the values given in Fig. 13 and the effect of the interior support. It can be seen that the effect of shrinkage is not negligible for the continuous composite beam. It is also apparent that the magnitude of the slab force induced by a shrinkage strain of 0.0002 is of the same order of magnitude as the force produced by live load on the member.

5. COMPARISON OF THEORY WITH EXPERIMENTAL RESULTS

5.1 General

The general numerical method of analysis was applied to several test beams to check its validity. Sufficient data was available from four beams[16,18] tested at Fritz Engineering Laboratory to demonstrate the applicability of the method. The influence of changes in the important variables which affect the behavior of continuous composite members could be studied by using the data available. From the studies made, suitable values of these variables could be derived for analysis of composite beams in general.

5.2 Composite Beams CC-3F and CC-4F

Each of the composite beams CC-3F and CC-4F was 50 ft.-10 in. long with two equal spans of 25 ft.-0 in. between supports (see Fig. 15). Symmetrical concentrated loads were applied 10 ft.-0 in. from the exterior support in each span. The two members consisted of a reinforced concrete slab 60 inches wide and 6 inches thick interconnected to a W21x62 steel beam by 3/4 inch stud shear connectors. The rolled beams were all supplied from ASTM A36 steel. Additional details of the continuous composite beams are shown in Figs. 10 through 12.

Two mathematical models were used to analyze the test beam CC-4F. One model represented a beam with a cracked slab in the negative moment region, and the other represented a beam with an uncracked slab throughout. The full length of CC-4F was divided into 125 elements to represent a cracked slab while the uncracked slab was represented by only 106 elements. The 19 additional elements of the first model represented cracks in the negative moment region at which only the longitudinal reinforcement was effective. These 19 elements were 0.1 inch in length to represent a crack and associated bond failure.

All elements were interconnected at nodal points located at stud connectors except in the negative moment region where connectors were omitted. Imaginary connectors were provided in this region in order to simulate friction between the beam and slab. The cracks were assumed to be at 6 inch intervals corresponding to the spacing of the transverse reinforcement. Due to symmetry of member and loading conditions the analysis could be completed with 63 simultaneous equations for the cracked slab model and 53 equations for the uncracked model.

The cracked slab model was developed first because it was felt that cracks had to be simulated in the analysis. However, this model could not be used for the inelastic analysis, and the second model was developed. Solutions were made with both models using the same slab stiffness for corresponding elements. It was found that both models produced the same results because the 19 additional

elements which represent cracks in the original model did not produce any significant effect in the behavior of the member as a whole. The stress-strain relationships for the concrete slab and steel beam as well as the load-slip relationships for connectors were defined on the basis of test data.

The stress-strain relationship for a cracked reinforced concrete slab in tension is not well defined. The limiting stiffness of the concrete slab in tension is the stiffness of the uncracked slab. As more and more cracks form the stiffness is reduced since the force required to produce a given elongation is reduced. The crack pattern is produced by shrinkage and loading and is not necessarily the same as the crack pattern which is produced in determinate members such as simple beams or tension specimens. A stress-strain curve for a given crack pattern may be represented by a curve similar to that of the uncracked slab with lower stiffness. A family of similar curves represent different crack patterns. Mathematically these curves can be described in terms of the properties of the uncracked curve by selecting a proper coefficient of lower value in place of the modulus of elasticity.

In this manner a stress-strain curve for the reinforced concrete in compression was modified and assumed to be representative of the average stress-strain curve of the slab in tension by merely decreasing the stiffness. Many computer solutions of beam CC-4F were studied to determine the effect of changing this and other variables. From this work a reasonable choice of a curve from the

family was made. When a drastic change in the amount of longitudinal reinforcement was made, another curve from the family was found that better described the properties of the slab. However, it was found from experience that the selection of a curve did not have to be very precise. At the same time the solution could be improved by trying different curves.

In the tests for determining the behavior of stud shear connectors in the regions of negative moment[19], it was reported that although the concrete was badly cracked in tension, the portions of concrete between the cracks carried up to a quarter of the total tension force applied to the slab. It was also shown[4] that the effective flexibility (i.e., extension at a given tensile force, or reciprocal of the effective stiffness) of the reinforced concrete slab was about half that of the reinforcement alone for average slab strains up to 0.5 percent. This provided a starting point for arriving at a suitable effective modulus of elasticity for the cracked slab.

In the future greater precision in predicting the behavior of continuous members might be achieved by a greater refinement in treating the slab in the tensile region and by further refinement of the load-slip relationships.

From the data on slab force and slip obtained from the beam tests, it was possible to select a load-slip relationship which was reasonable for each region of the member.

From the mathematical models that were used for the analysis of the continuous composite beams it was possible to determine the proper value for the effective stiffness of the concrete slab in tension by matching the slab force with the experimental results at the interior support.

The slab force variation over one span of CC-4F is shown in Fig. 16. The solid curve represents the solution for a stiffness of 20 percent of the uncracked slab, and the dotted curve represents the solution if one considers only the reinforcing steel in the negative moment region. Static load-slip curves were used for both solutions and the full effective stiffness was employed for the positive moment region. The two curves deviated near the dead load point of contraflexure and result in quite different values at the interior support. It can be seen that the slab force was very low compared to experimental results for the participation of only the longitudinal reinforcement in the negative moment region. The correlation with test results in the positive moment region was very good.

Figure 17 shows the slab force distribution obtained by using unloading load-slip curves. These unloading load-slip curves which are associated with the effect of load cycling give lower slab forces both in the positive and the negative moment regions. This can be seen by comparing Figs. 16 and 17. The curve of Fig. 17 does not produce a suitable solution for the positive moment region.

Figure 18 shows the calculated deflection curves for beam CC-4F obtained using two different load-slip relationships. The solid line in Fig. 18 was obtained if one adds deflection due to shear to the lower curve obtained using the loading load-slip relationship. This curve passes through the test result. Obviously the total deflection obtained by adding deflection due to shear to the other curve results in predicted deflections which are much too large. Therefore the best overall correlation was obtained from using the load-slip relationship obtained during loading. The unloading load-slip relationship was useful in simulating the deterioration of the member produced by two million cycles of fatigue loading. Thus the middle curve of Fig. 18 represents the deflection due to bending at the end of the fatigue test.

The bottom curve in Figs. 19 and 20 was obtained by considering that only the longitudinal reinforcing steel was effective in the negative moment region. The stiffness assumed for friction in the region without connectors was 100 kips per inch of slip for a 6 inch length of slab. The other four curves that appear in Figs. 19 and 20 were obtained by using 20 percent of the stiffness of the uncracked slab for the slab in the negative moment region. The middle curve of each figure was obtained by using the unloading load-slip curves. It is obvious that the bottom curve in these figures does not correlate well with the test data.

The upper curve of Fig. 20 seems to represent the best correlation with the test data at zero cycles. This curve was obtained

by increasing the friction in the region without connectors. The upper curve of Fig. 19 could be altered to fit better in the same manner. The data for the test indicates that the friction force was much higher at the start of testing than at two million cycles. One can also obtain results that are closer to the test results by varying the stiffness of the slab.

From a study of Figs. 19 and 20 one gains an appreciation for the behavior of the member in the negative moment region. Initially the effectiveness of the slab is relatively large because the slab has few cracks and the friction force is high. As cracks form friction, slab stiffness, shear connector stiffness, and slab force all decrease. For application to bridge design it is necessary to consider a solution which describes the average behavior between zero cycles and failure. Reasonable assumptions for the variables are available from the curves of Figs. 19 and 20. Many solutions other than those that have been represented have been made. Some of these exhibit better correlation with test results. However, considering the margin of error in test data, variations in behavior from one member to another and the uncertainty that exists with regard to material properties and the effect of shrinkage, it is doubtful that a greater precision than the selection of a reasonable combination of assumptions can be justified. A sound approach is to make two solutions that will provide upper and lower bounds.

The two upper curves of Fig. 20 can be considered as bounds of the solution. This provides excellent characterization of behavior

in the region of the shear connectors. The spread between the curves at the support is large, but this could be improved by increasing the friction stiffness of the lower curve.

The force on the shear connectors can be easily obtained from the curves of Fig. 20 as the difference in the slab force at any two adjacent points. Since the force per connector for a fatigue life of two million cycles should not exceed 4.4 kips per connector, it can be seen that the force on the end connector early in the test was too high. This is to be expected since connectors were designed considering only the reinforcing steel in the slab and neglecting the effectiveness of the slab.

From the results presented in Figs. 19 and 20 it is obvious that the average stiffness of the cracked slab in tension was at least 20 percent of the stiffness of the uncracked slab. The friction stiffness was in the upper range of 100 to 500 kips per inch of slip for a 6 inch length of slab. These values are valid for longitudinal reinforcing steel percentages of approximately one percent. If the longitudinal reinforcing steel is reduced so that the steel yields at the crack, the stiffness of both the slab and the friction must be reduced to obtain a satisfactory solution. This will be illustrated by considering member CC-3F which had 0.66 percent of longitudinal reinforcing steel.

Because of the deterioration of member CC-3F due to fatigue loading, it was possible to compare theoretical results with test data for only the initial static test. In Fig. 21 the lower curve

gives the computer solution for only the reinforcing steel while the upper curve was obtained using 12 percent of the uncracked slab stiffness. The friction stiffness was 100 kips per inch of slip for a 6 inch length of slab. The test points correlate well with the upper curve.

The change in the percentage of longitudinal reinforcing steel from 0.66 percent for CC-3F to 1.03 percent for CC-4F resulted in nearly doubling the stiffness of the cracked slab and increasing the friction stiffness by four times. The governing factor producing this change in behavior is the fact that the steel yields at a crack in CC-3F and does not yield in CC-4F. It is also of importance that the cracked slab of CC-3F was considerably stiffer than the reinforcing steel alone.

5.3 Continuous Composite Beams CC-1F and CC-2F

Beams CC-1F and CC-2F which were tested earlier at Fritz Engineering Laboratory had the same dimensions and longitudinal slab reinforcement as CC-3F. Beam CC-2F had connectors spread over the negative moment region except for a length of 22 inches on each side of the interior support while CC-1F had no connectors in the negative moment region.

The slab force in the negative moment region of CC-2F is shown in Fig. 22. The lower curve shows the result from considering only the longitudinal reinforcement, and the upper curve was obtained using a slab stiffness of 12 percent of the uncracked slab stiffness with the static load-slip curves. The static test point is well above

the upper curve while the test point for two million cycles is well below this curve. The slab force at the interior support for this member is considerably greater even after two million cycles than was the initial slab force in CC-3F. This indicates that spreading the connectors over the negative moment region produced a greater stiffness for the cracked slab. It was found that initially the stiffness of the slab was about 20 percent, but the amount by which the slab stiffness changed during the test was significant.

At the time that CC-2F was tested, it came as a surprise that shear connectors midway between the center support and the dead load point of contraflexure failed in fatigue. In all previous tests, the end connectors of a group had failed first. However, Fig. 23 shows that the computer solution predicts that the maximum force on the shear connectors occurred in the region where failed connectors had been found. Figure 23 also reveals that the slab force was considerably above the desirable level of 4.4 kips per connector. Although spreading of the connectors produces more complete composite action in the negative moment region, it has the undesirable aspect of requiring more connectors. The discontinuity of the slab force is again due to the change from one load-slip curve to another at the point of contraflexure.

Beam CC-1F offered the greatest challenge for simulation by the mathematical model because it had no connectors in the negative moment region and had no connectors provided to develop forces in this region. Figure 24 shows the results for an early static test and the computer solutions. The upper curve was again obtained with a slab

stiffness of 12 percent and the lower curve resulted from considering only the longitudinal reinforcing steel. The test result is only slightly higher than that predicted by the upper curve. It is obvious that the shear connector forces are very high considering the change in slab force that takes place at each connector location at the right of the curve.

The results obtained for beams CC-1F and CC-2F greatly increased confidence on the validity of the mathematical model for simulating the behavior of a continuous composite beam. It is apparent that one can study the effect of changing any variable while holding the others fixed by using the mathematical model.

5.4 Prestressing the Slab in the Negative Moment Region

Relatively small tensile stresses due to shrinkage or loading can produce cracking in the slab of composite beams. In order to make the concrete slab effective and reduce the size and number of cracks to a minimum in the negative moment region, it may be beneficial to prestress the negative moment region.

The advantages to be gained from prestressing the slab are:

1. Cracking of the slab due to shrinkage and live load can be controlled.
2. Slab participation in the negative moment region can be increased to 100 percent.

3. Fatigue failure of the top flange of the steel member due to the presence of welded shear connectors can be avoided.
4. Fatigue of shear connectors due to uneven distribution of connectors can be avoided.
5. The amount of longitudinal reinforcing steel required to produce satisfactory slab performance in the negative moment region can be greatly reduced.
6. It should be possible to reduce deterioration of the slab by controlling cracking.

The primary disadvantages of prestressing the concrete slabs would be the increased cost and additional inspection required to ensure proper installation and prestressing. Since the prestressing of slabs is common in Europe, the technology for this type of work is available, but the methods in use would have to be modified for use here. The region between the prestressed slab and the reinforced slab may present construction problems. The development of a large prestressing force will require more shear connectors than a reinforced slab in the negative moment region.

The effect of prestressing the slab can be determined by the method of analysis under consideration. In analyzing the effect of prestressing, the moment due to loading and the strain induced by prestressing should be considered at the same time if non-linear load-slip curves are used for the shear connectors.

As an example consider a prestressed composite beam with a span of 15 ft.-0 inches. The beam consists of a prestressed concrete slab 60 inches wide and 6 inches thick interconnected to a W21x62 steel beam by 3/4 inch stud shear connectors 4 inches high. The spacing of connectors was 5 inches with connectors in pairs. Symmetrical concentrated loads of 35.56 kips were applied 7 ft.-5 inches from the interior support. A prestressing force of 250 kips was applied at the centroid of the concrete slab at both ends. Details of the prestressed composite beam are shown in Fig. 25.

Figure 26 shows the slab force induced in the prestressed composite beam. The upper curve is the slab force due to prestressing with 250 kips whereas the lower curve is the value due to the combined effect of prestressing and external loads. In this analysis the stiffness of the slab was taken as the stiffness of the uncracked slab and the load-slip relationship was a loading curve. Loss of prestressing as shown in Fig. 26 was small and increased from both ends to the interior support. It is also apparent that the loss of prestressing is due to the elastic shortening only in Fig. 26. Other prestressing loss could be considered in the same manner.

5.5 Inelastic Analysis of Beam CC-4F

The two-span continuous composite beam CC-4F was analyzed by assuming constant dead load points of contraflexure, i.e. the reaction forces of the three supports of the member were proportional to the externally applied load. Slab forces and deflections of the

beam were found by superimposing the values of each increment load. When the stiffness of the beam due to the non-linearity of material was changed significantly with the member forces, the deflection at the interior support may not be zero by assuming constant points of contraflexure. It is interesting to observe the effect of the change in stiffness of beam CC-4F on the interior support deflection.

Figure 27 shows the slab force distributions of the half length of beam CC-4F. Four curves of slab force distributions were shown due to various externally applied loads of 90, 120, 150, and 180 kips.

Figure 28 shows the deviation of the deflection at the interior support produced by assuming constant points of contra-flexure. The deviation is practically zero until the externally applied load reaches 100 kips. This means that stiffness of the member may be considered as constant up to the load level of 100 kips. Beyond this critical value the stiffness was changing significantly with increasing applied load. The member forces and the reactions of the three supports of the beam are no longer linearly proportional to the externally applied load.

The actual values of the slab forces may be found by a trial and error method when the externally applied load is over 100 kips. The reactions of the supports could be assumed due to each increment of load. Moment could be calculated from the assumed reactions and member forces and deflections could then be evaluated. The deflection at the interior support would be checked to see if the value was within some specified tolerance limit. Once the reactions were found,

the slab forces and connector loads were found for the particular increment of load. Another approach to the solution is to make a support settlement correction to the computer solution based on the deflections given in Fig. 28. This avoids the trial and error procedure but may not produce as good a solution for large deflections.

The effect of shoring was not considered in this solution. For unshored members it is merely necessary to take into account the initial strains and stresses of the steel beam due to the dead load. Figure 29 shows the slab force distributions in the negative moment region which is an enlarged portion of Fig. 27 for the negative moment region. The slab force distributions due to an externally applied load of 60 kips are also shown in Fig. 29 for reference. The ultimate load of beam CC-4F was 177 kips and the slab force based on the average yield strength of 45 ksi[16] for the longitudinal reinforcement was 165 kips. A good correlation can be observed.

6. DESIGN CONSIDERATIONS

6.1 Magnitude of Longitudinal Reinforcement

In all of the test beams, except CC-4F, the amount of longitudinal reinforcing steel in the slab over the negative moment region was essentially the amount required by the 1969 AASHO Specifications. None of these beams performed satisfactorily although beam CC-2F was better than beams CC-1F and CC-3F. Beam CC-4F exhibited satisfactory behavior due to the increased participation of the concrete slab in the negative moment region. This was brought about primarily by increasing the percentage of longitudinal slab steel to about one percent. This amount of longitudinal reinforcement successfully controlled cracking due to shrinkage. Beam CC-4F also exhibited a relatively ideal crack pattern after cyclic loading with none of the cracks being larger than desirable[16].

One guide line which provides an obvious lower bound for the percentage of longitudinal reinforcement in any region of a continuous beam where the slab will be in tension under live load is that the maximum tension force that can be developed in the concrete should not be sufficient to yield the steel when the slab cracks. This is necessary to control the size of cracks and to retain the effectiveness of the concrete after cracking at a level corresponding

to composite behavior of the concrete and reinforcing steel. If the steel yields, only a tie bar remains at the crack and composite behavior decreases while the danger of a disastrous result such as was experienced in beam CC-3F can develop.

From the tests of continuous composite beams it has been shown that the amount of longitudinal reinforcing steel should be greater than the minimum required by the 1969 AASHO Specifications. Beam CC-4F provides an apparently satisfactory design. Therefore, it is reasonable to recommend that the minimum amount of longitudinal reinforcing steel should be one percent of the area of the concrete slab over the negative moment region. This seems like a considerable amount of steel, but in continuous reinforced concrete bridges a greater amount of steel is actually placed in the slab over interior supports, thus providing effective crack control.

The size of the longitudinal reinforcing bars should be as small as practical and well distributed in the cross-section of the concrete slab in the negative moment region in order to maximize their effect in crack control. This also serves to increase the effective area of the slab. Stresses in the negative moment region of continuous composite beams should be computed using the section properties determined with the actual stiffness of the slab and incomplete interaction. However, in practice or for design purposes the stresses may be evaluated on the basis of the actual reinforcing steel area neglecting the concrete slab with complete interaction as specified by the 1969 AASHO Specifications (Section 1.7.97).

6.2 Number of Shear Connectors

Continuous composite beams designed by the latest AASHO Specifications may be composite or non-composite in the negative moment region. In practice the majority of continuous composite bridges have been designed without shear connectors in the negative moment region. When shear connectors are omitted in the negative moment region, a tie-bar force is developed in the longitudinal reinforcement extending from the negative moment region. In order to prevent a premature fatigue failure of the shear connectors near the inflection points, the AASHO Specifications (Section 1.7.101(a)(3)) require that additional shear connectors should be provided to take the additional force.

When continuous composite beams are designed composite in the negative moment region the number of shear connectors according to the current AASHO Specifications should be based on the area of longitudinal reinforcement. Elastic theory may be used to calculate the range of horizontal shear per inch of the member.

$$S_r = \frac{V_r Q}{I} \tag{6.1}$$

Where S_r is the range of horizontal shear per inch of the member, Q is the statical moment of the area of longitudinal reinforcement in the negative moment region. I is the moment of inertia of the composite cross-section, V_r is the range of shear. Enough shear connectors are also needed to insure that the static ultimate strength of the

composite beam can be achieved. In general a bridge structure is usually governed by fatigue requirements.

The results of testing three beams exhibiting shear connector failure points to the fact that the number of shear connectors being provided was not sufficient[16,18]. The magnitude of the slab force determined by the method developed in this study was consistently greater than that determined by considering only the reinforcing steel. This fact was also observed in a previous experimental study[16,18]. Therefore, the number of shear connectors must be determined for a larger force. From the point of view of design the number of shear connectors provided must be computed on the basis of the area of the longitudinal steel plus some percentage of the area of the concrete slab.

It was found that in beam CC-4F, which had an amount of longitudinal steel of 1 percent in the negative moment region, the effective stiffness of the cracked concrete slab in tension was approximately 20 percent of the uncracked slab in compression[16]. The British Codes of Practice, Part 2 specifies that shear connectors shall be computed on the basis of the total area of the concrete slab in the negative moment region[7]. The percentage of the area of the concrete slab is really a compensation for the effective stiffness of the cracked slab in tension.

It seems reasonable to recommend that shear connectors should be computed on the basis of 20 percent of the area of the

concrete slab or the longitudinal steel area plus 12 percent of the area of the concrete slab, whichever gives the higher value. In design the concrete slab should be transformed to an equivalent area of steel by means of the proper modular ratio of steel to concrete. Elastic theory may be used to calculate the range of horizontal shear stress per inch of the member.

$$S_r = \frac{V_r\ Q'}{I} \qquad (6.2)$$

Where Q' is the statical moment of the transformed area determined as suggested above. I is the moment of inertia of the composite cross-section. The other section properties should be consistent with the value used for calculating Q'. V_r is the range of shear. Figure 30 shows the number of additional connectors required using the current AASHO Specifications as a basis for possible values of the effective area of concrete slabs.

6.3 Spacings of the Shear Connectors

The pattern of shear connectors influences the effectiveness of the concrete slab. This provides the reason for the relatively good performance of beam CC-2F compared to CC-1F and CC-3F which had the same amount of longitudinal steel. In beam CC-2F the shear connectors were spread out over the negative moment region to a greater extent. The computer analysis showed the same trend toward a relatively better performance from spreading connectors. Beam CC-4F was superior to CC-2F, but the behavior of CC-4F could have been

improved by spreading the connectors over a larger portion of the negative moment region.

In order to avoid the possibility of fatigue failure in the tension flange of the steel section at points where shear connectors are welded, the connectors have to be shifted from the region of maximum negative moment toward the dead load point of contraflexure. On the other hand, in order to achieve the maximum effectiveness of the concrete slab the shear connectors have to be spread out over the negative moment region as much as possible. Therefore, it is reasonable to recommend that the spacing of the shear connectors should be a maximum as long as the fatigue failure of the tension flange can be prevented. The additional stiffness attributed to the slab by the proposed changes in design procedure will make it possible to have connectors nearer to the interior support.

7. SUMMARY AND CONCLUSIONS

A method for the analysis of a continuous composite beam with a discrete shear connection has been presented. The analysis is based on incomplete interaction between the slab and the beam, and considers inelastic behavior of the slab, beam, and shear connection. The analysis can be extended to consider the effect of shrinkage and a prestressing force in the concrete slab.

The basic assumptions involved in the analysis are that the slab and the beam deflect equally at all points along the spans and that the strain distribution in the slab and the beam are linear, though not necessarily continuous across the interface. On the basis of these assumptions, equilibrium and the compatibility conditions, a set of simultaneous equations has been derived with the unknowns as the axial force in the slab and the beam. Direct methods of solving the equations with the aid of a computer have been employed even for the inelastic range. The method of analysis has been made as general and as flexible as possible such that a wide variety of practical problems can be solved.

The theoretical results for cracked slabs in the negative moment region have been compared with the experimental results of laboratory tests of four continuous composite beams. Satisfactory correlation has been obtained between a computer analysis and the

experimental values for slab force, loads on shear connectors, and the strain distribution in the cross-section.

A comparison of the results obtained from the computer and experimental studies of continuous composite beams has led to the following conclusions.

1. The mathematical model developed in this investigation can be used to analyze continuous composite beams. The effect of shrinkage of the concrete and prestressing of the slab can be evaluated along with the effect of live load.

2. The important variables that affect the behavior of the negative moment region have been found to be the number and size of the reinforcing steel and the number and spacing of the shear connectors.

3. The actual stiffness of the cracked concrete slab in the negative moment region can be determined on the basis of 20 percent of the area of the concrete slab or the longitudinal steel area and 12 percent of the area of the concrete slab for members having a longitudinal reinforcement of 1 percent or less.

4. The number of shear connectors provided for the negative moment region should be determined using the actual stiffness to prevent fatigue failure of connectors.

5. The actual stiffness of the slab is increased when shear connectors are spread as far as possible over the negative moment region.

6. Stresses in the negative moment region should be computed using the section properties determined with the actual stiffness of the slab in complete interaction. For design purposes complete interaction may be assumed, and stresses may be calculated using the actual reinforcing steel area neglecting the concrete area.

APPENDIX A

NOMENCLATURE

Subscripts s and b used with notation means slab and beam respectively.

Index i used with notation means for each element (i) of the composite beam, for nodal point i, or for each element of the matrix whichever is applicable.

Prime used with notation means for each increment of externally applied load.

A, B	Constants determined from pushout test
$\{A\}$	Column matrix or vector A
A_s, A_b	Cross-sectional area
B_i	Bottom diagonal element of tridiagonal matrix
B_{ij}	An element of matrix B
C_s, C_b	Distances between the respective centroidal axes of the slab and the beam and the interface between the slab and the beam.
$\{C\}$	Column matrix or vector C
d	Intercept on the slip axis of the tangent to the load-slip curve
D_i	Diagonal element of tridiagonal matrix
E_s, E_b	Moduli of elasticity of materials
F_i	Horizontal direct force acting at the centroids of the slab and the beam for element (i)

APPENDIX A (continued)

I_s, I_b	Moments of inertia
K	Slope of the load-slip curve of a connector or stiffness of a connector
K_h, K_v	Spring constants in x- and y-directions respectively
M	External bending moment applied to the composite beam
M_s, M_b	Resisting bending moments
q_c, Q_i	Connector loads
ΔS, ΔX, S	Length of the element
T_i	Top diagonal element of tridiagonal matrix
u, v	Components of displacements in rectangular coordinates
u_i	Displacement of nodal point i
x, y	Rectangular coordinates
y_i	Deflection of the composite beam
Z	Distance between the centroidal axes of the slab and the beam ($Z = C_s + C_b$)
α, β	Parameters for the cross-section of the composite beam
γ	Slip of a connector
γ_{xy}	Shearing-strain component in rectangular coordinates
ϵ_b, ϵ_{bt}	Unit elongation or strain at top of the beam
ϵ_s, ϵ_{sb}	Unit elongation or strain at bottom of the slab
ϵ_{sh}	Unit elongation or strain for shrinkage of concrete, or initial strain

APPENDIX A (continued)

ϵ_x, ϵ_y	Unit elongations or strains in x- and y-directions
σ_s, σ_b	Normal components of stress
σ_x, σ_y	Normal components of stress parallel to x- and y-axes
τ_{xy}	Shearing-stress component in rectangular coordinates
ϕ_s, ϕ_b	Curvatures

APPENDIX B

References for development of mathematical model and computer solution.

(a) Salvadori and Baron
NUMERICAL METHODS IN ENGINEERING, Prentice-Hall, Inc., New Jersey, 1962, 2nd Edition.

(b) Clough, R. W.
THE FINITE ELEMENT METHOD IN STRUCTURAL MECHANICS, Chapter 7 of STRESS ANALYSIS, Ed. O. C. Zienkiewicz and G. S. Holister, Wiley, 1965

(c) Zienkiewicz, O. C. and Cheung, Y. K.
THE FINITE ELEMENT METHOD IN STRUCTURAL AND CONTINUUM MECHANICS, McGraw-Hill, 1967

(d) Schultchen, Erhard G. and Celal N. Kostem
USER'S MANUAL FOR CSTES FINITE ELEMENT PROGRAM, Fritz Engineering Laboratory Report No. 237.58, June 1969

References for development of load-slip relationships for shear connectors.

(a) Slutter, R. G. and Driscoll, G. C.
FLEXURAL STRENGTH OF STEEL-CONCRETE COMPOSITE BEAMS, Journal of the Structural Division, ASCE, Vol. 91, No. ST2, April 1965

(b) Slutter, R. G.
THE FATIGUE STRENGTH OF SHEAR CONNECTORS IN STEEL-CONCRETE COMPOSITE BEAMS, Fritz Engineering Laboratory Report No. 316.9, September 1966

(c) Ollgaard, J. G.
THE STRENGTH OF STUD SHEAR CONNECTORS IN NORMAL AND LIGHTWEIGHT CONCRETE, Fritz Engineering Laboratory Report No. 360.4, May 1970

(d) Teraszkiewicz, J. S.
STATIC AND FATIGUE BEHAVIOR OF SIMPLY SUPPORTED AND CONTINUOUS COMPOSITE BEAMS OF STEEL AND CONCRETE, Engineering Structures Laboratories, Civil Engineering Department, Imperial College, London, September 1969

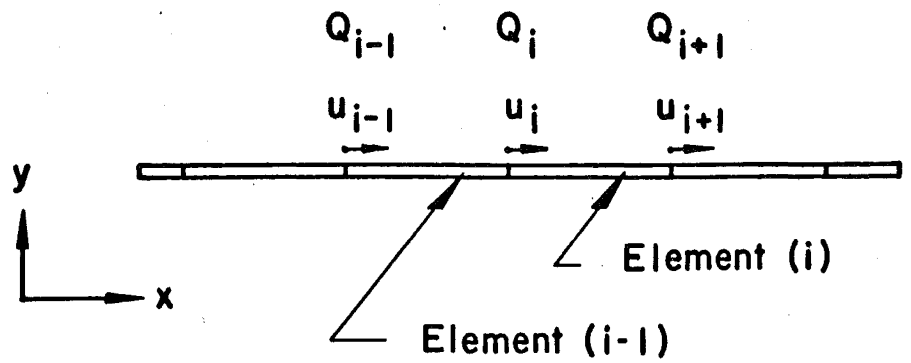

(a)

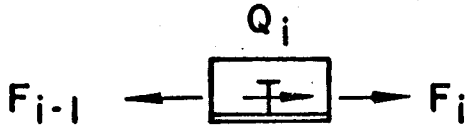

(b)

Fig. 1 Nodal Displacements

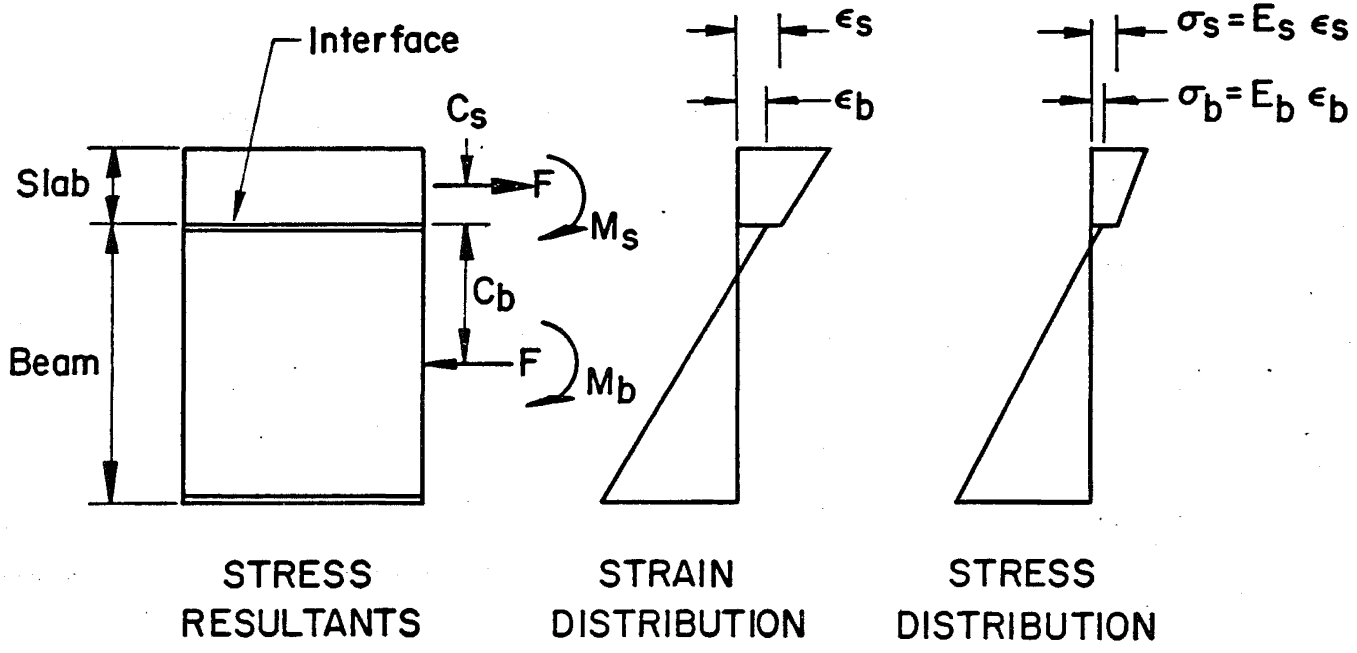

Fig. 2 Stress-Strain Distribution on Cross-Section

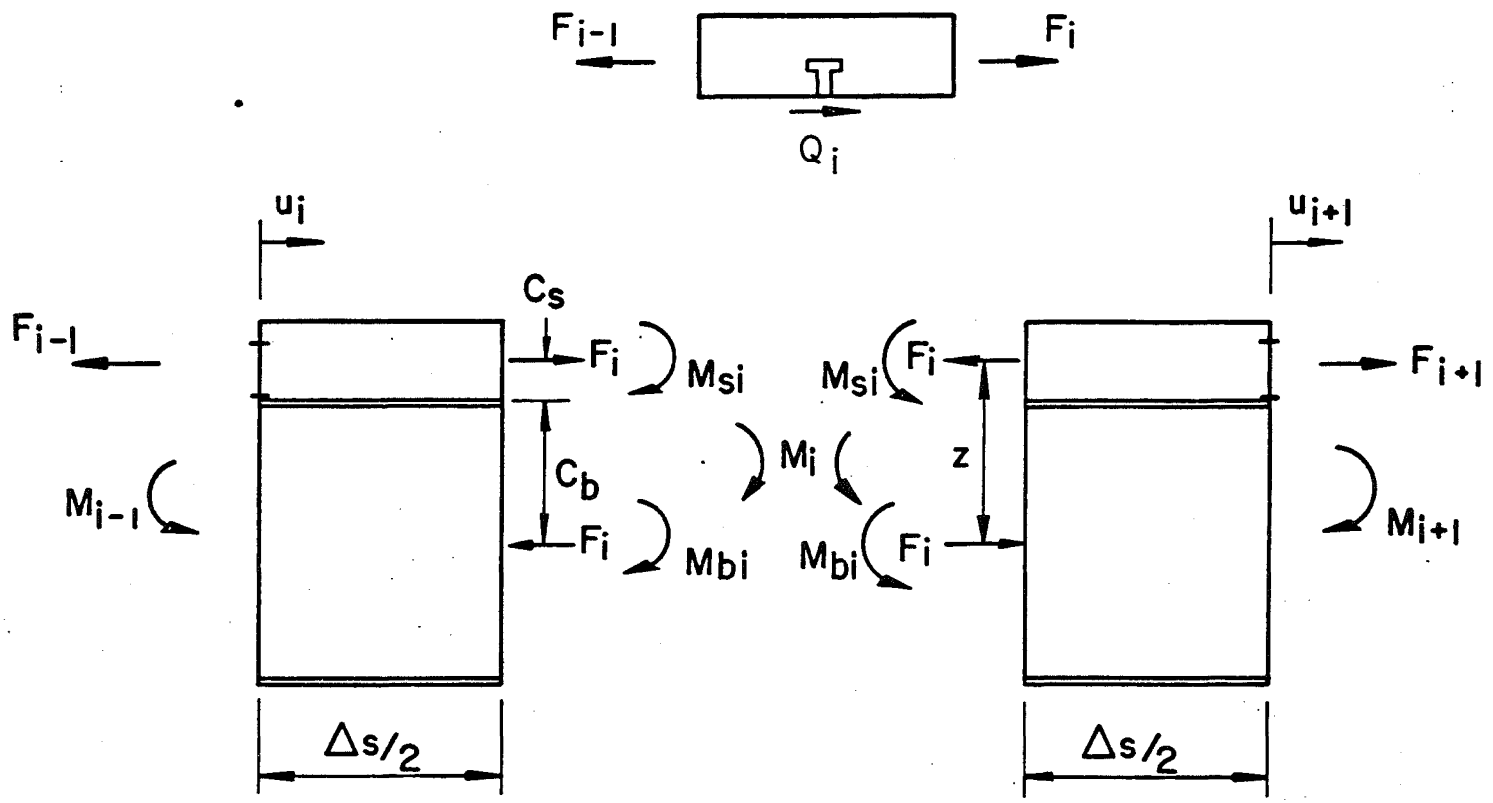

Fig. 3 Stress Resultants Acting at Element (i)

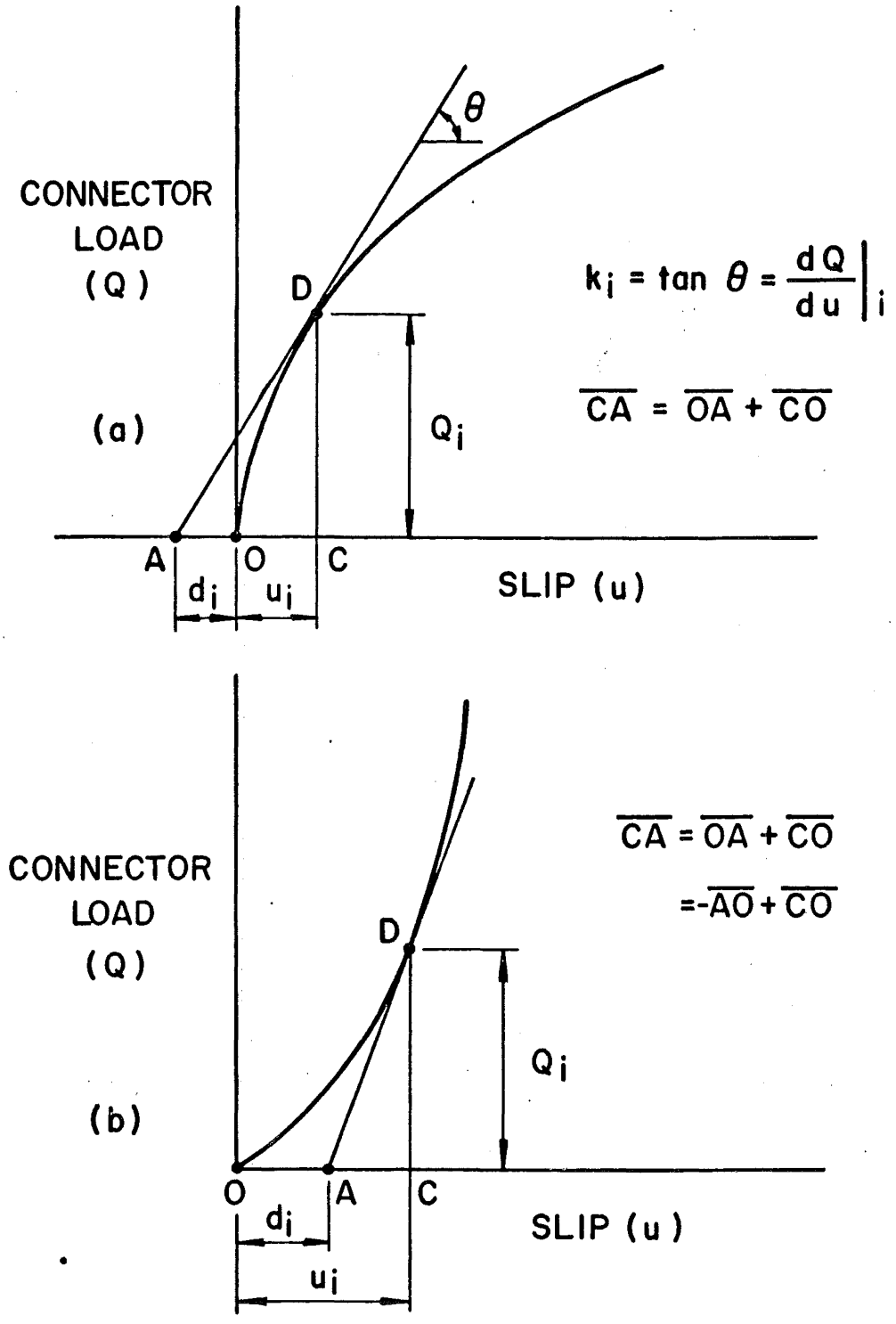

Fig. 4 Load-Slip Relationships for Connectors

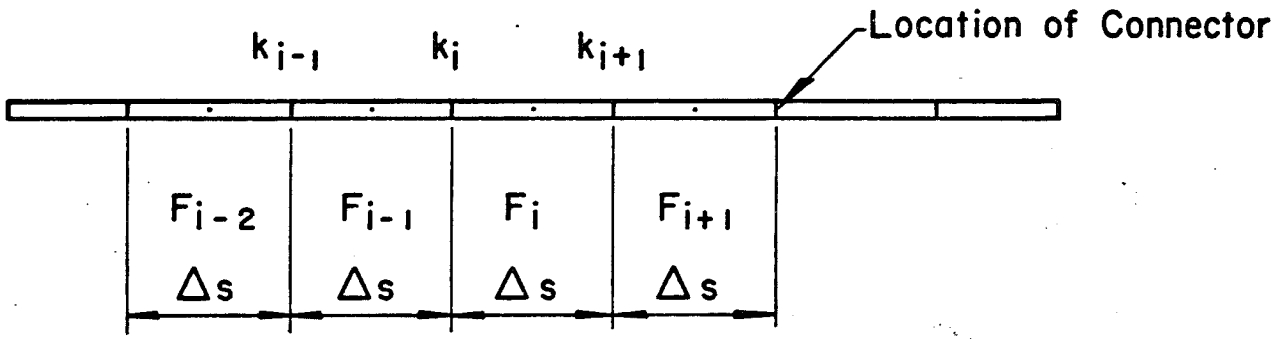

Fig. 5 Idealization of Composite Beam for Finite Difference Analysis

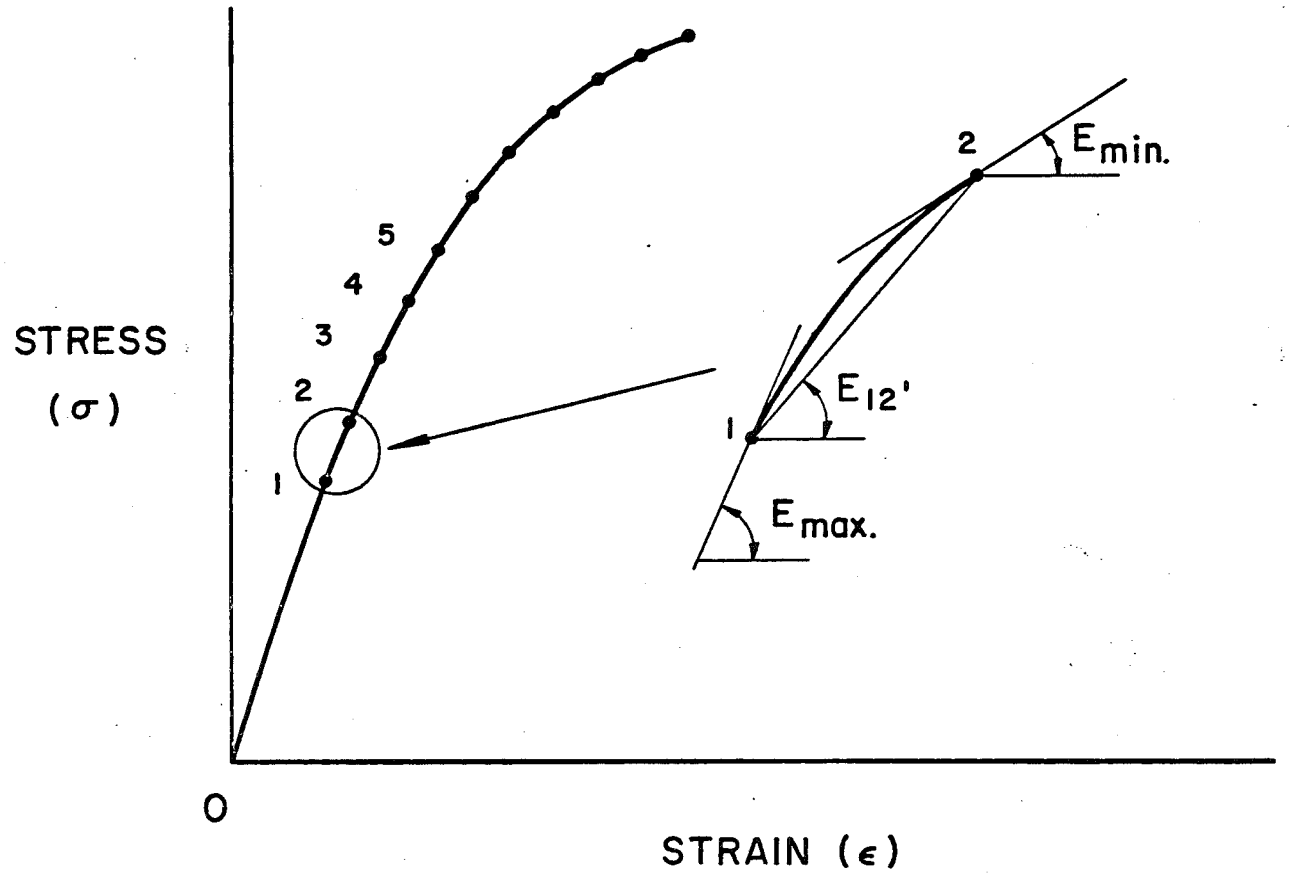

Fig. 6 Stress-Strain Relationship

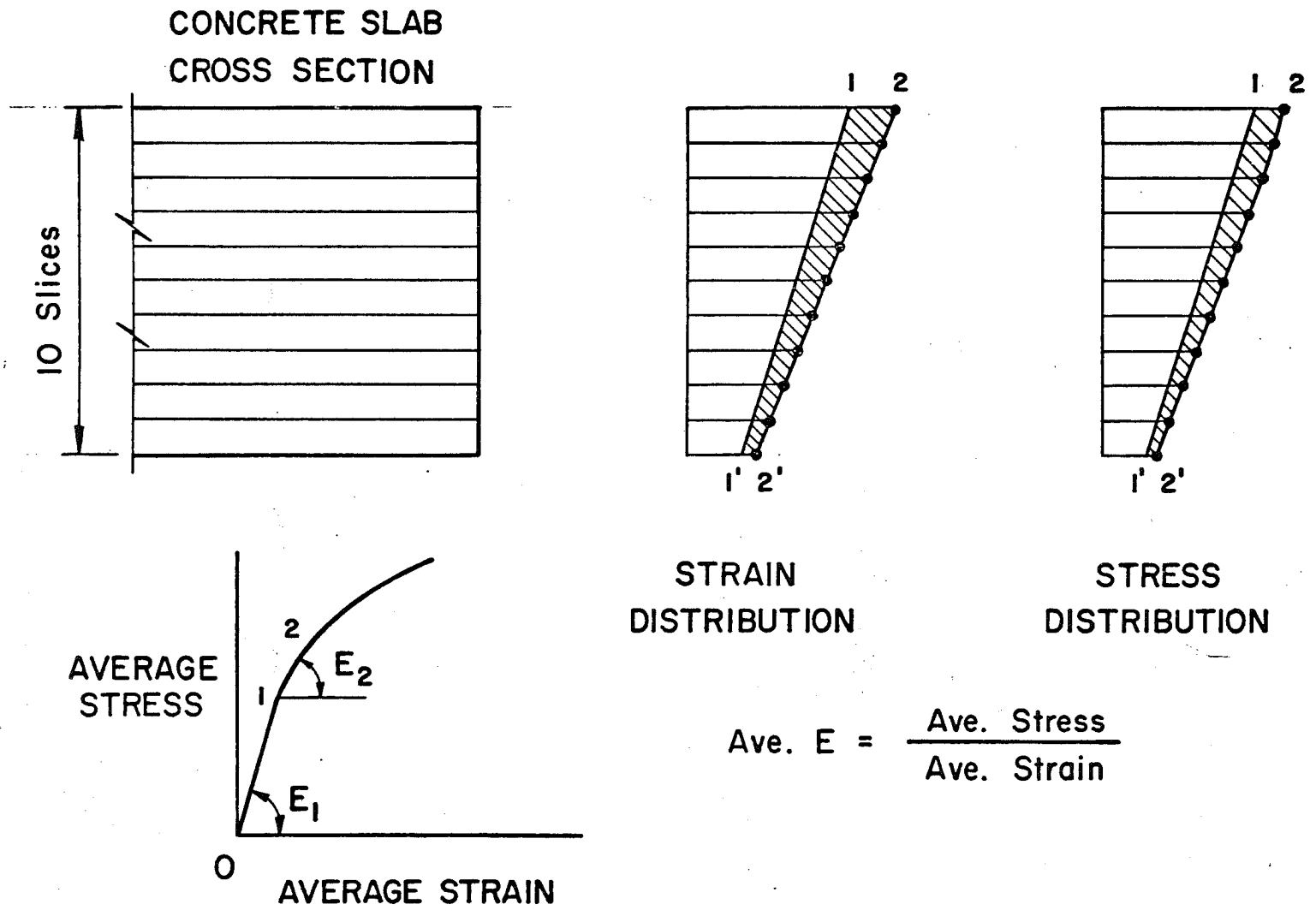

Fig. 7 Stress-Strain Distributions in the Concrete Slab

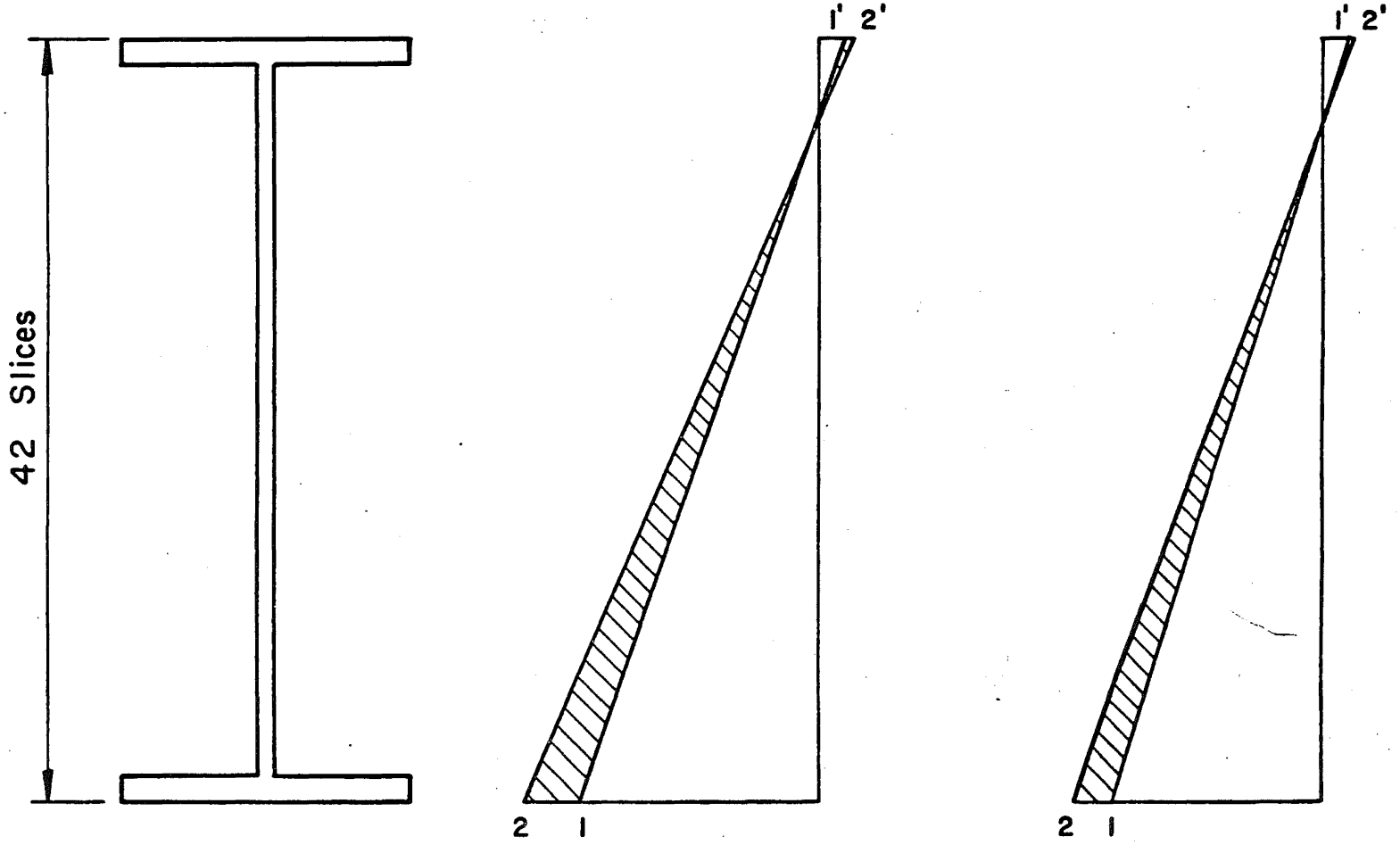

Fig. 8 Stress-Strain Distributions in the Steel Beam

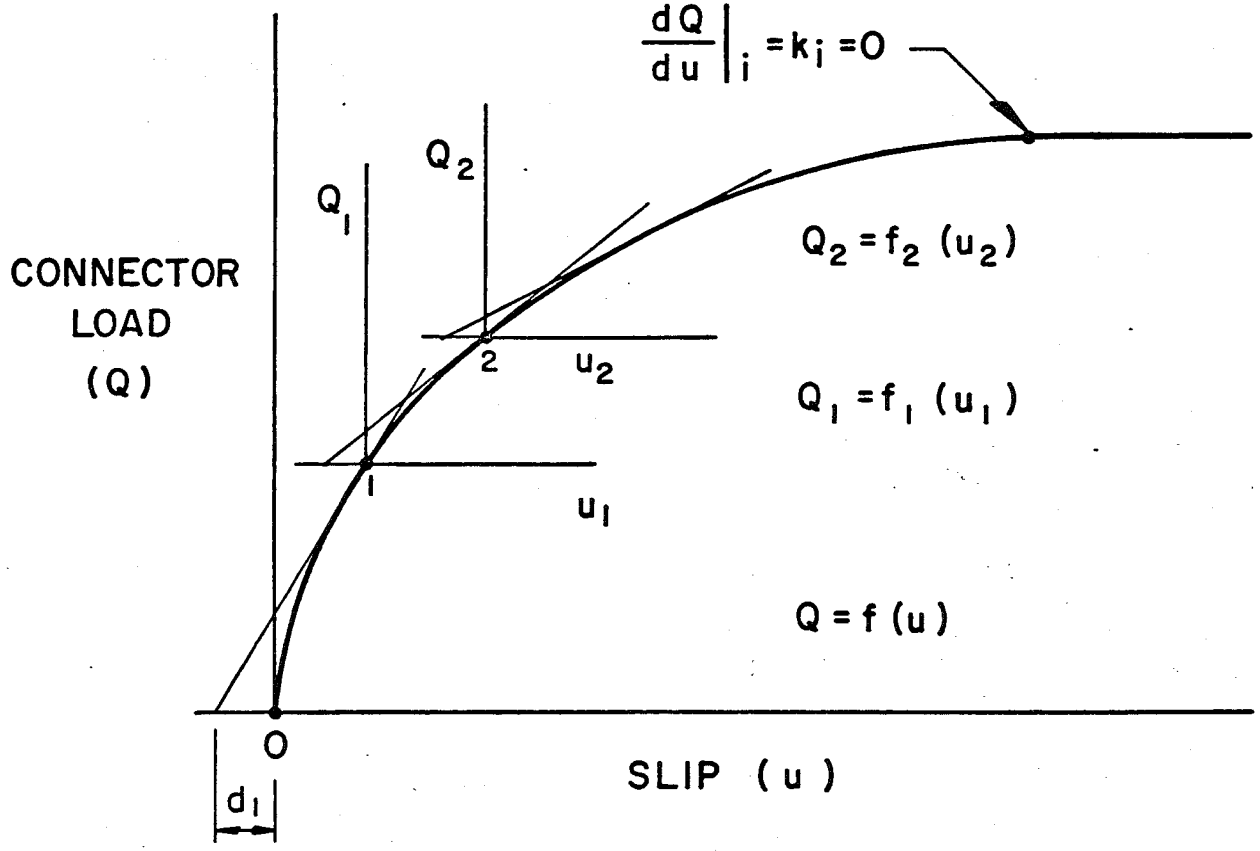

Fig. 9 Load-Slip Relationship for Different Coordinates

(a) CC-3F

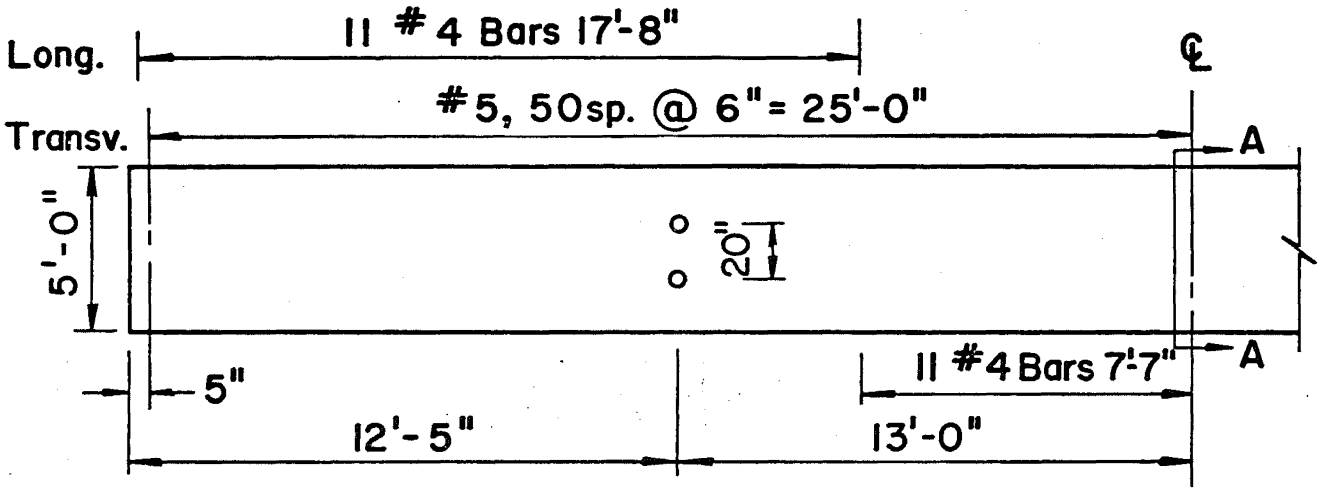

(b) CC-4F

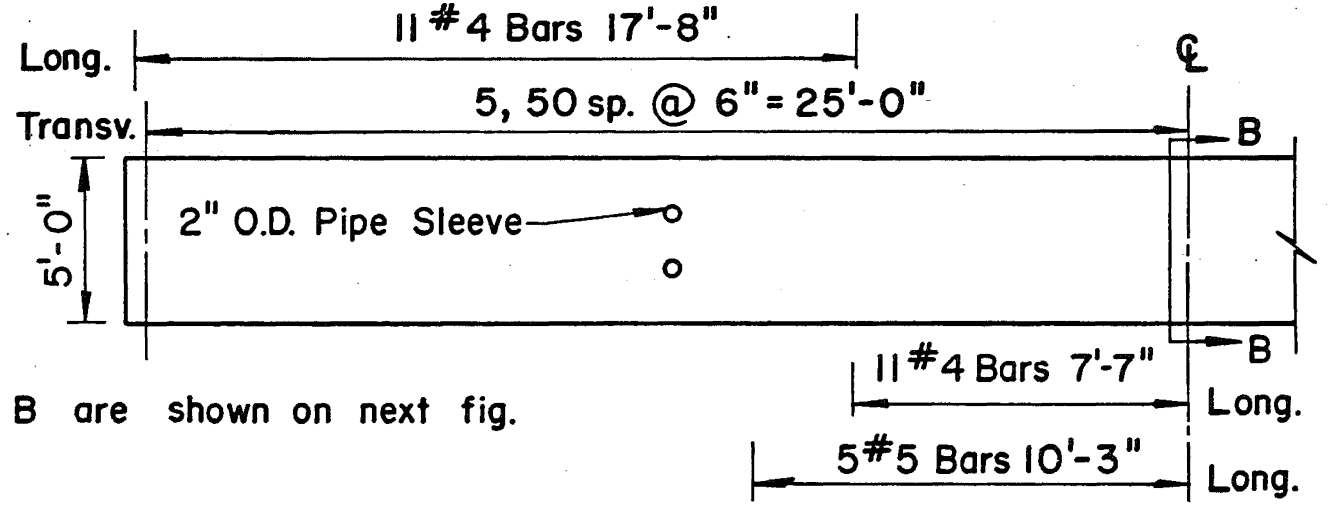

Sections A and B are shown on next fig.

Fig. 10 Details of Composite Beams of CC-3F and CC-4F

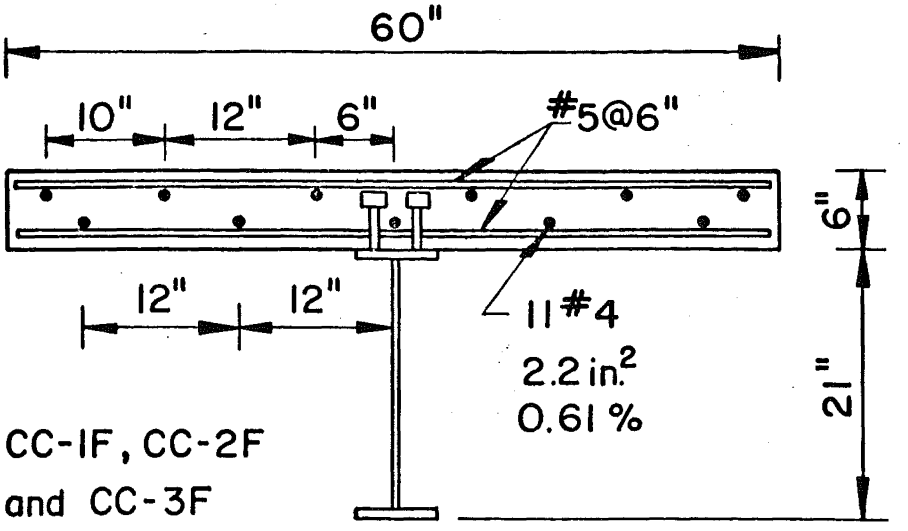

Section A

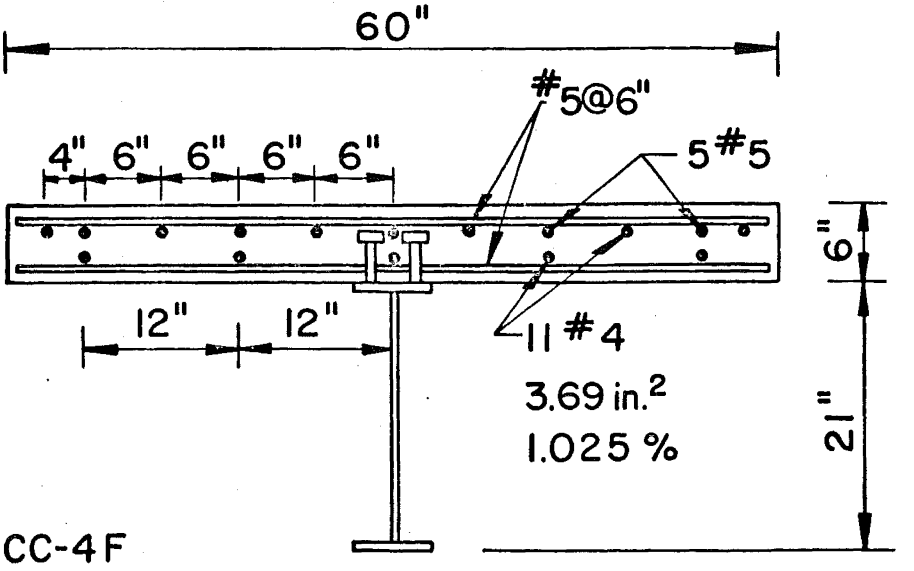

Section B

Fig. 11 Typical Test Beam Cross-Sections

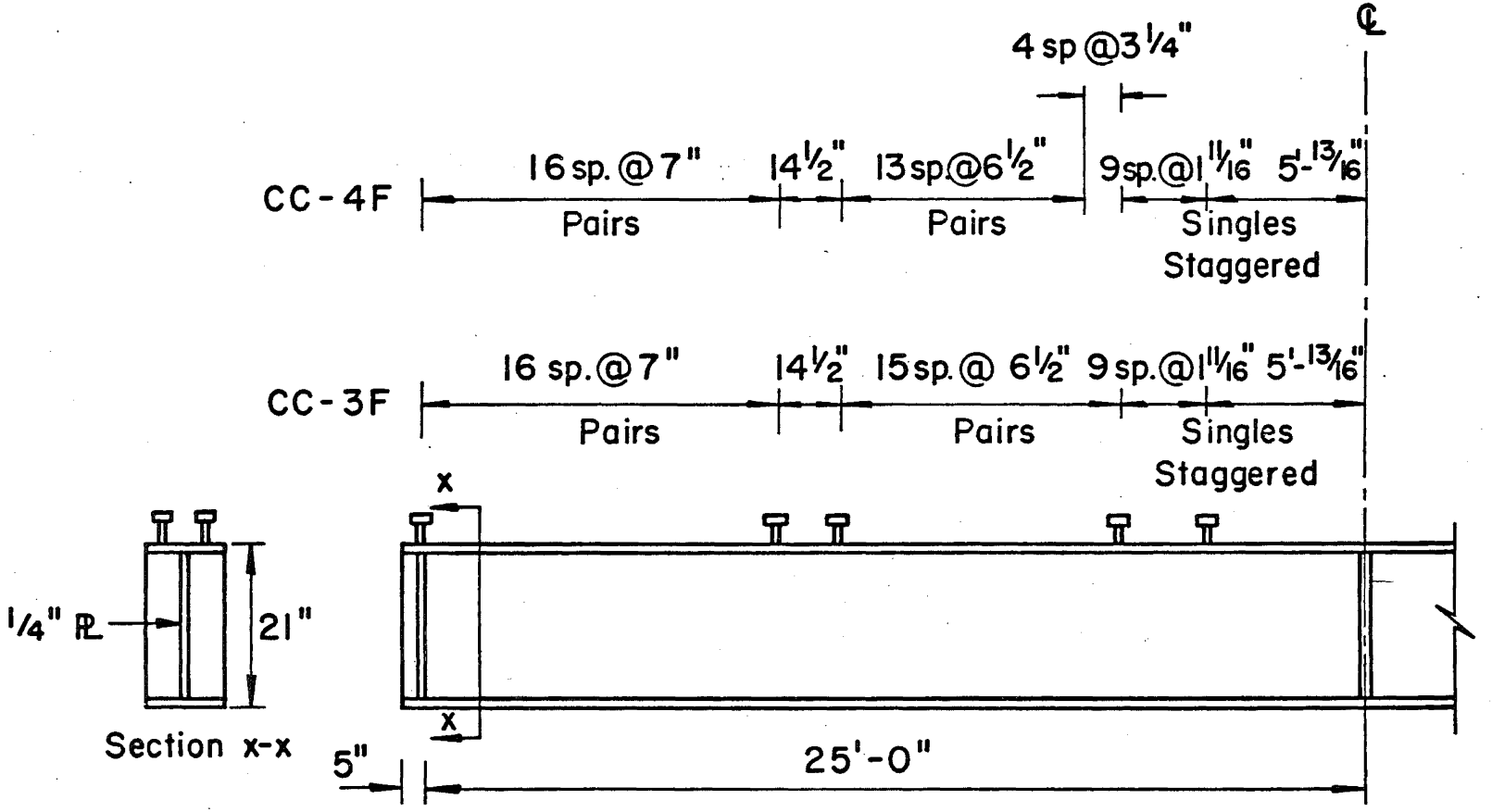

Fig. 12 Details of the Steel Beams For CC-3F and CC-4F

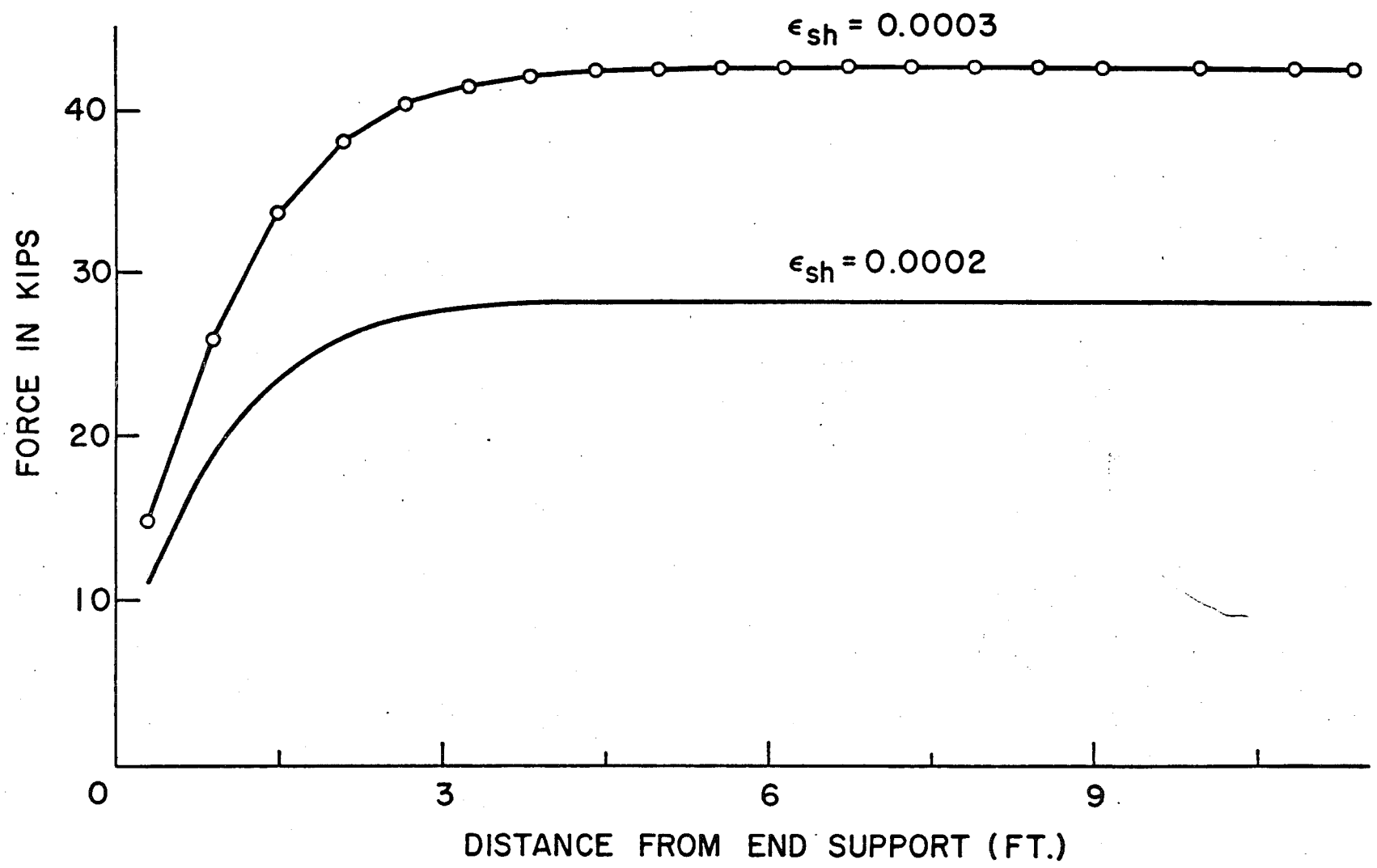

Fig. 13 Slab Force Due to Shrinkage for a Simple Beam

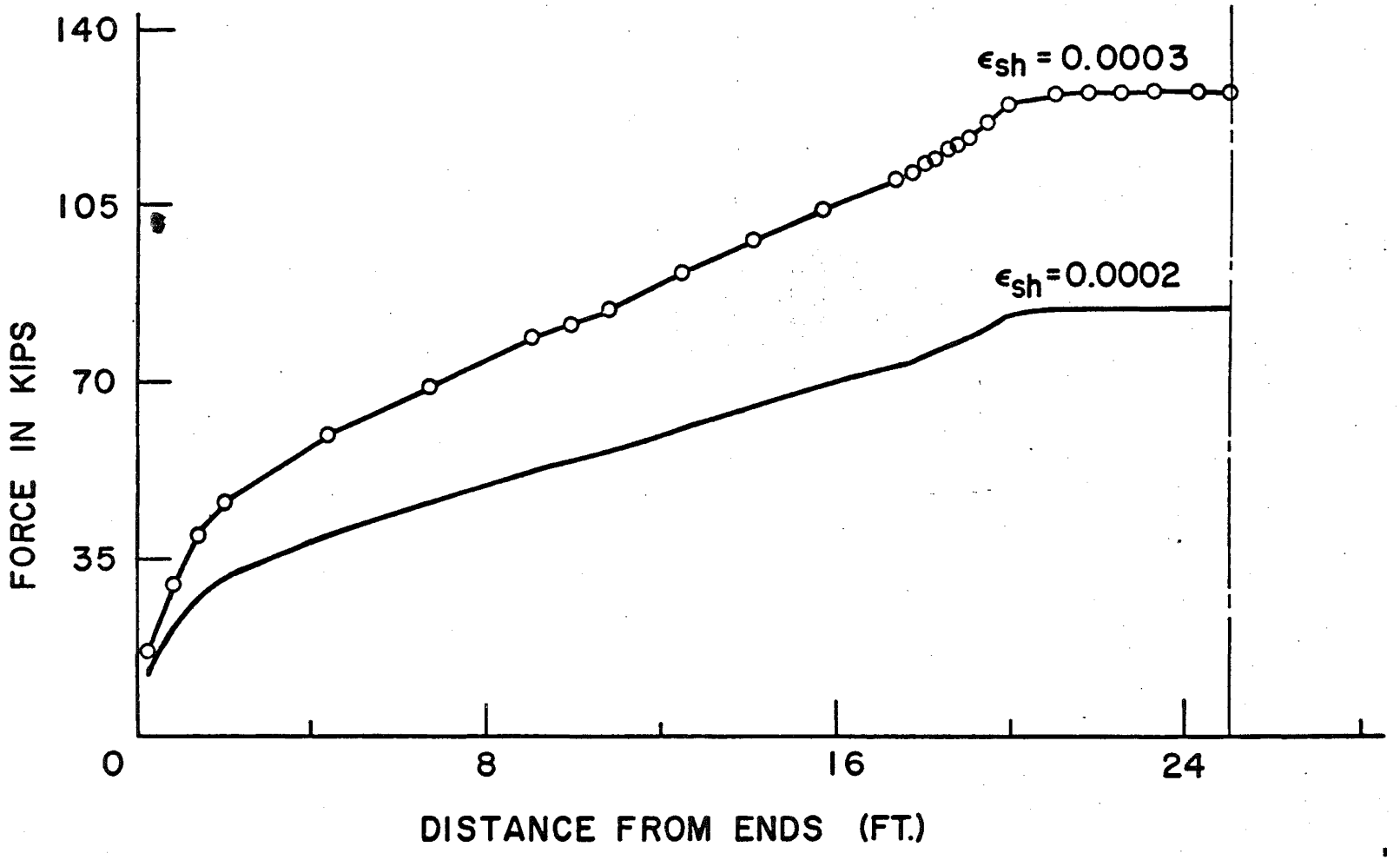

Fig. 14 Slab Force Curve Due to Shrinkage for Beam CC-4F

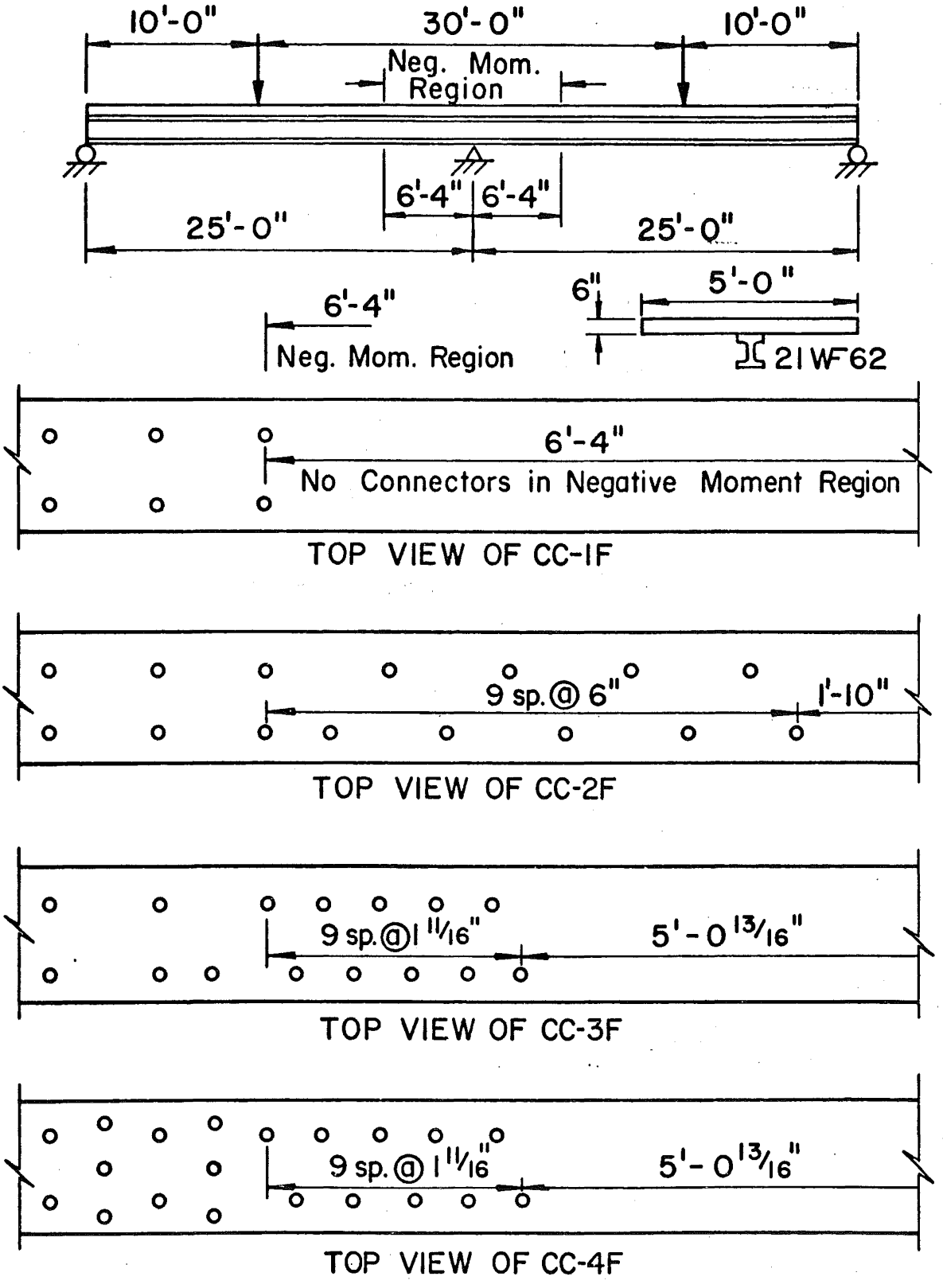

Fig. 15 Shear Connector Spacing in Negative Moment Region of Two Span Continuous Beams

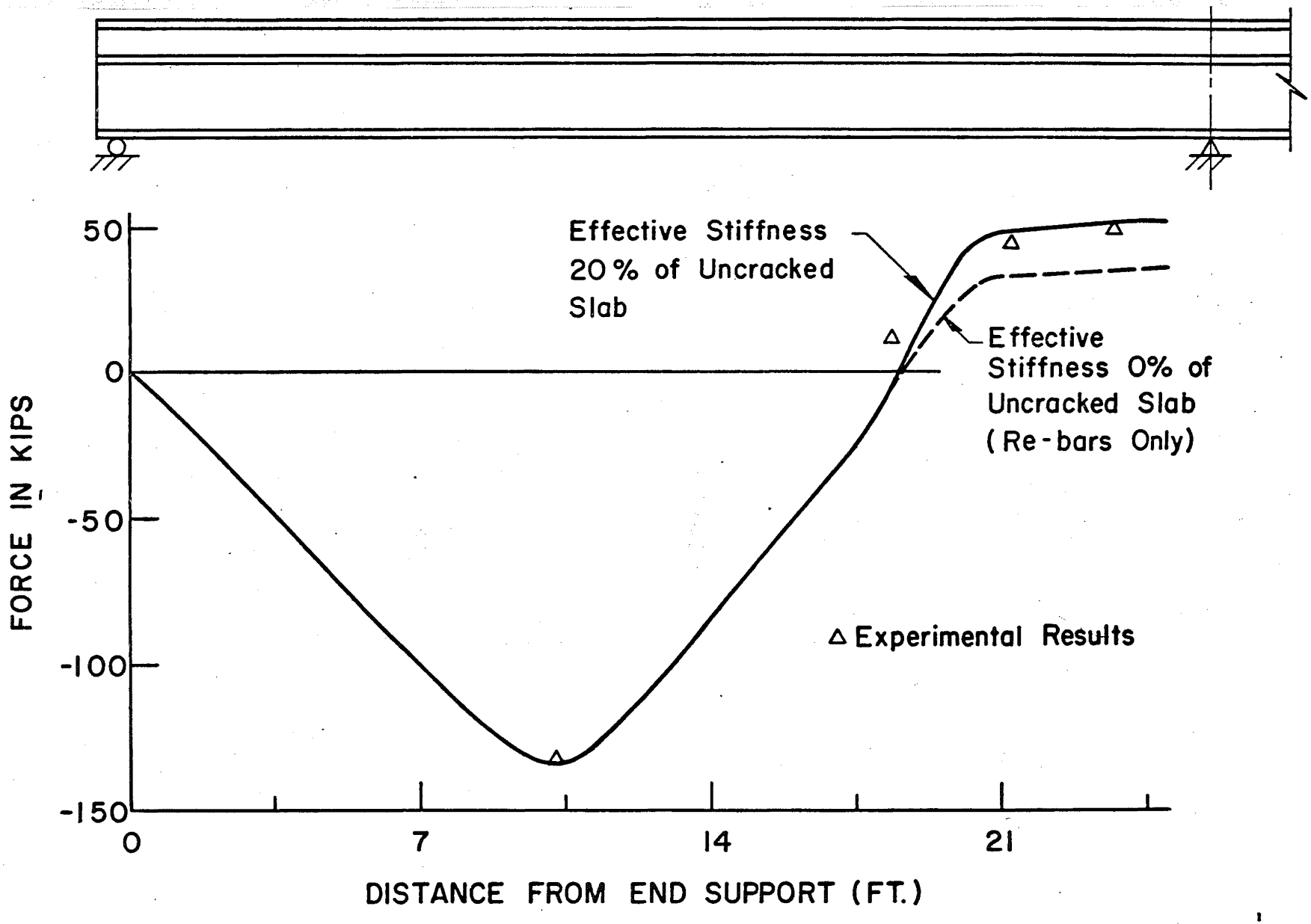

Fig. 16 Slab Force Distribution of CC-4F for Static Curve

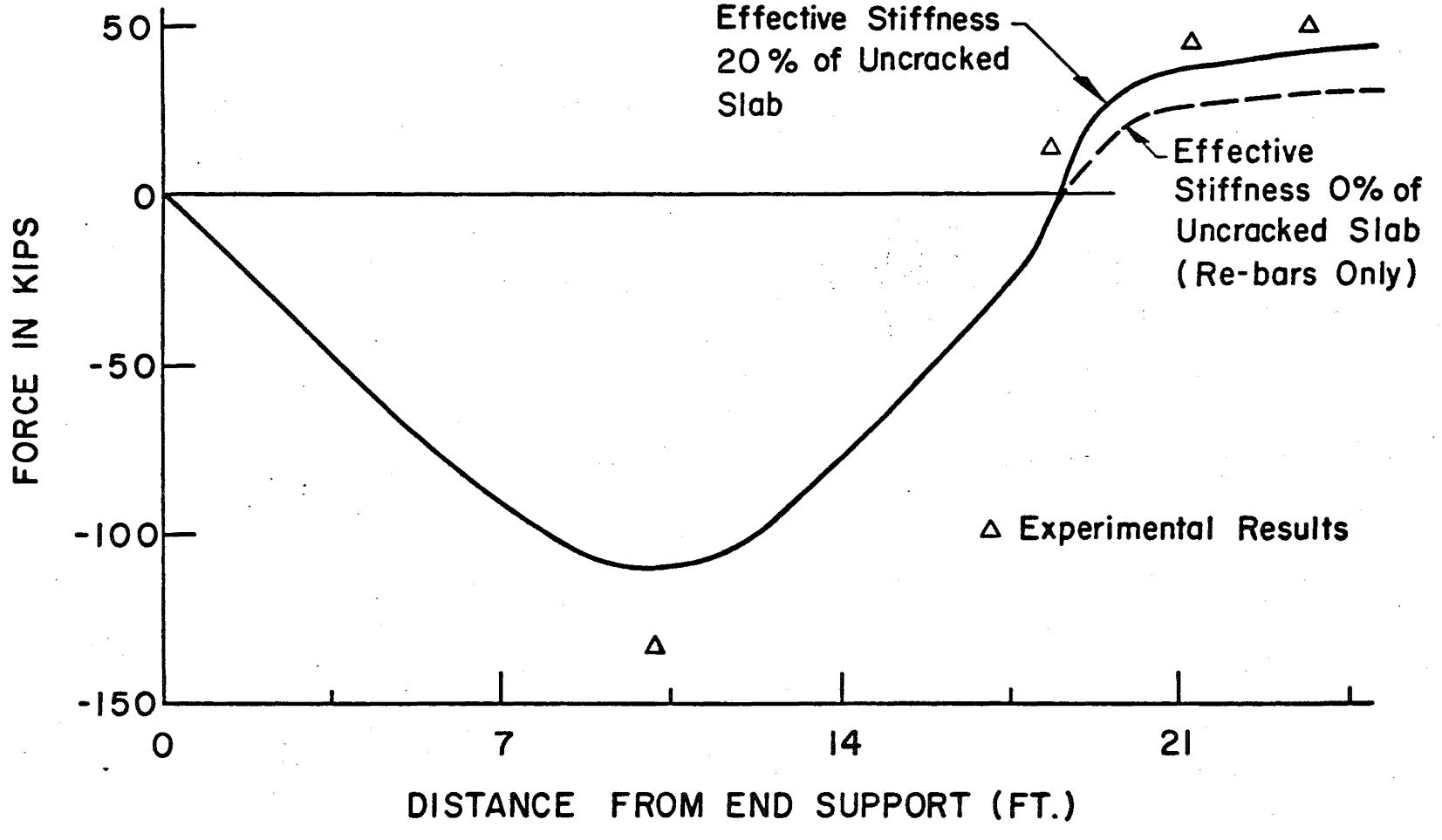

Fig. 17 Slab Force Distribution of CC-4F for Unloading Curve

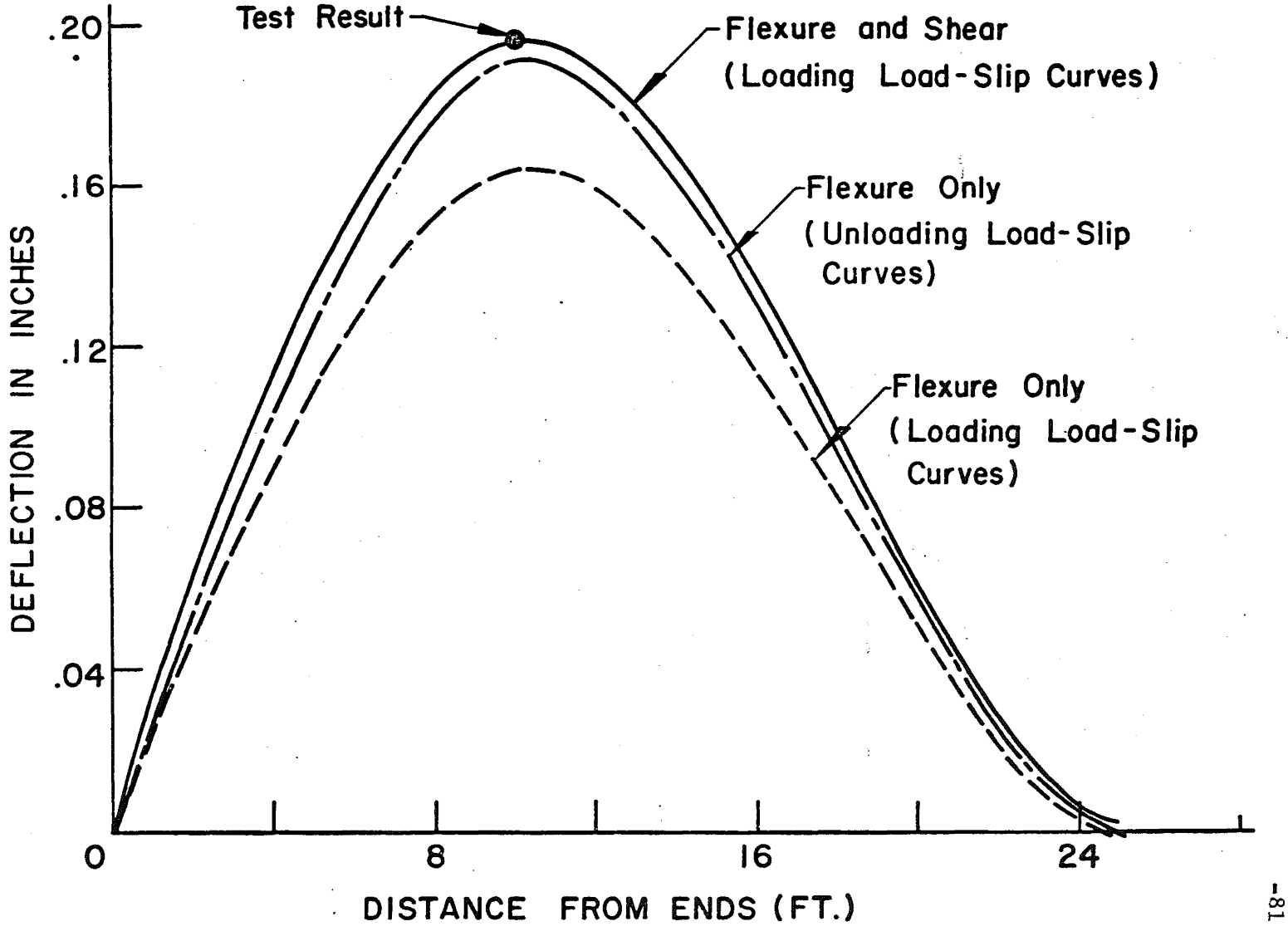

Fig. 18 Deflection Curves for Beam CC-4F

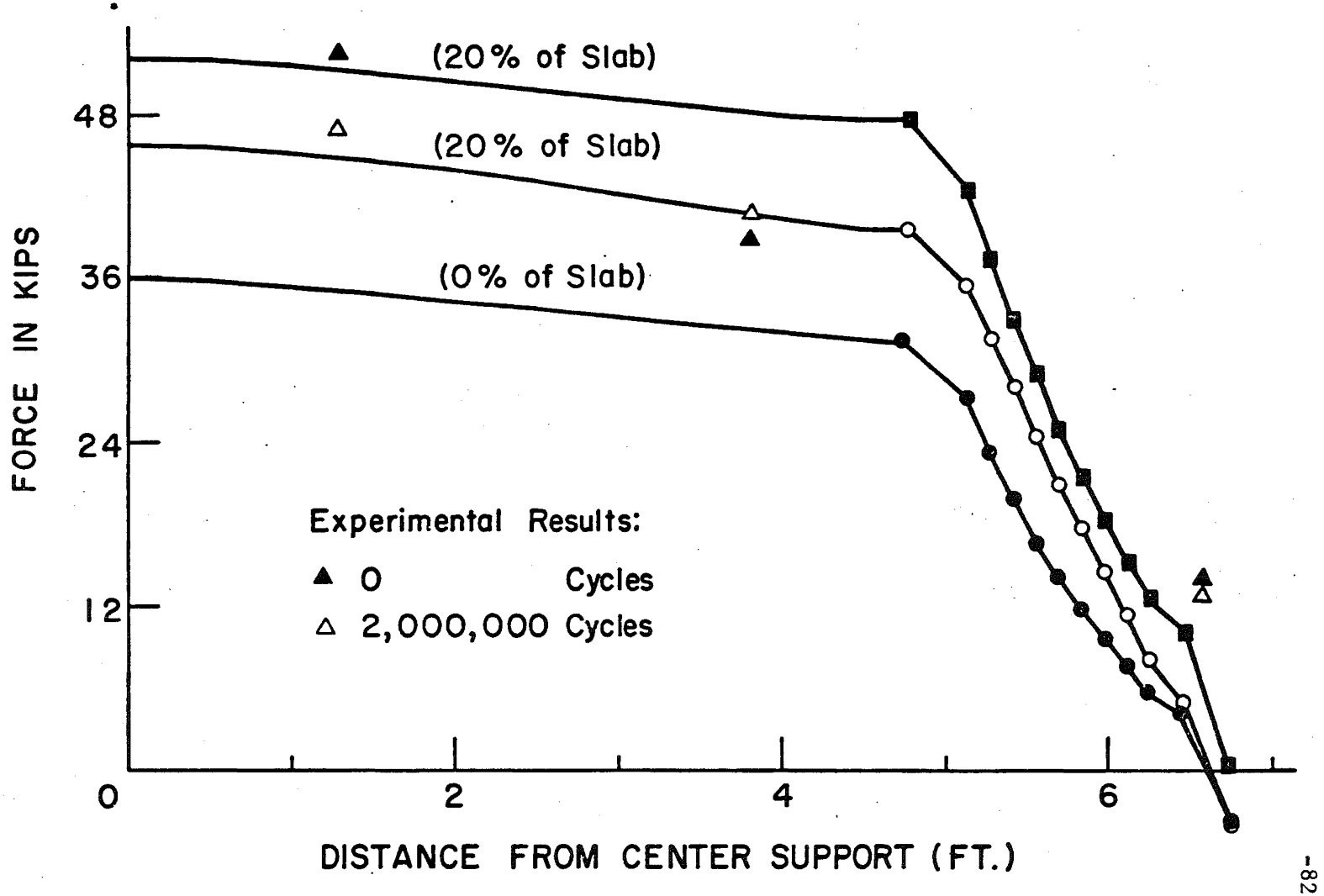

Fig. 19 Slab Force Curve for Beam CC-4F

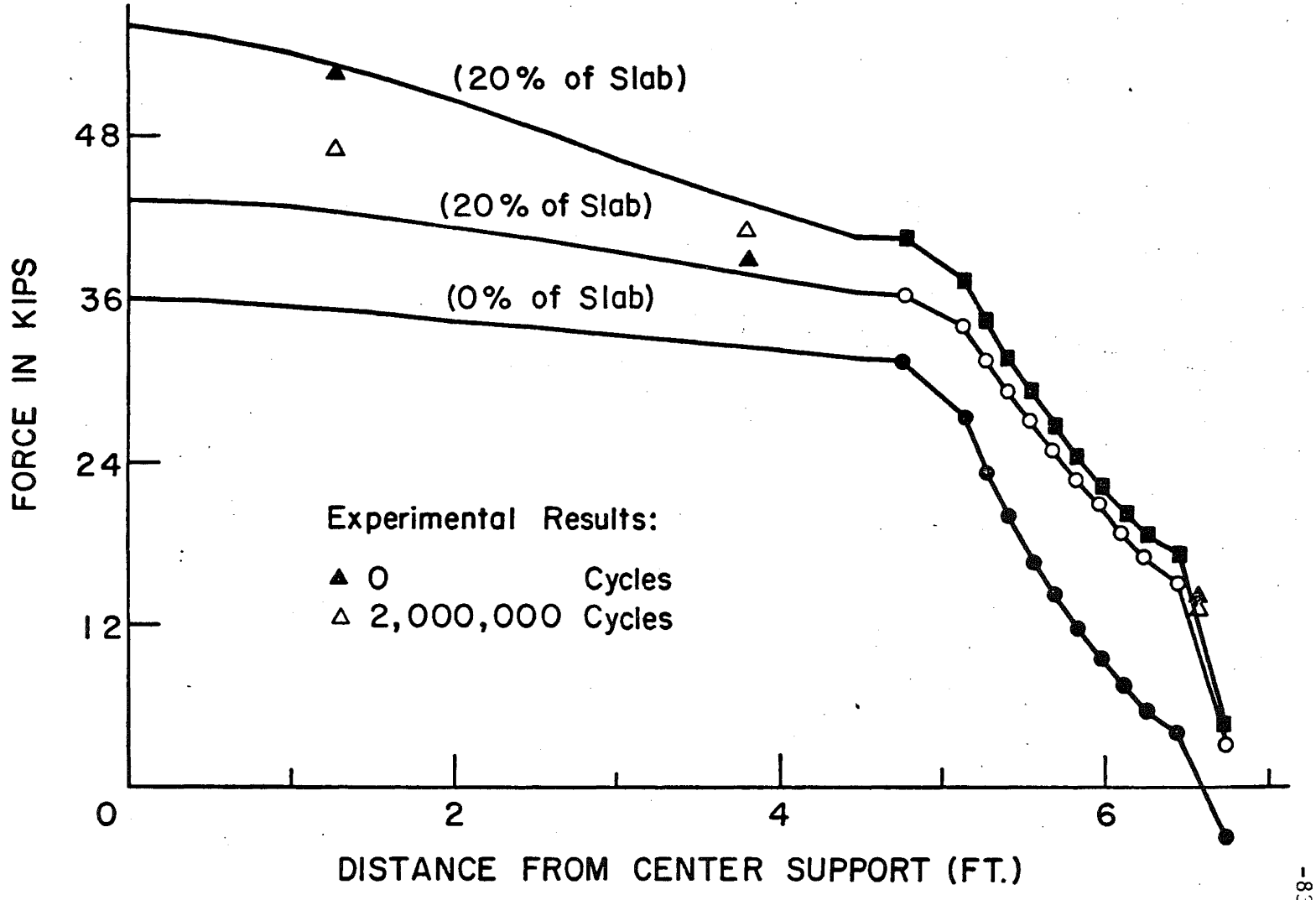

Fig. 20 Slab Force Curve for Beam CC-4F

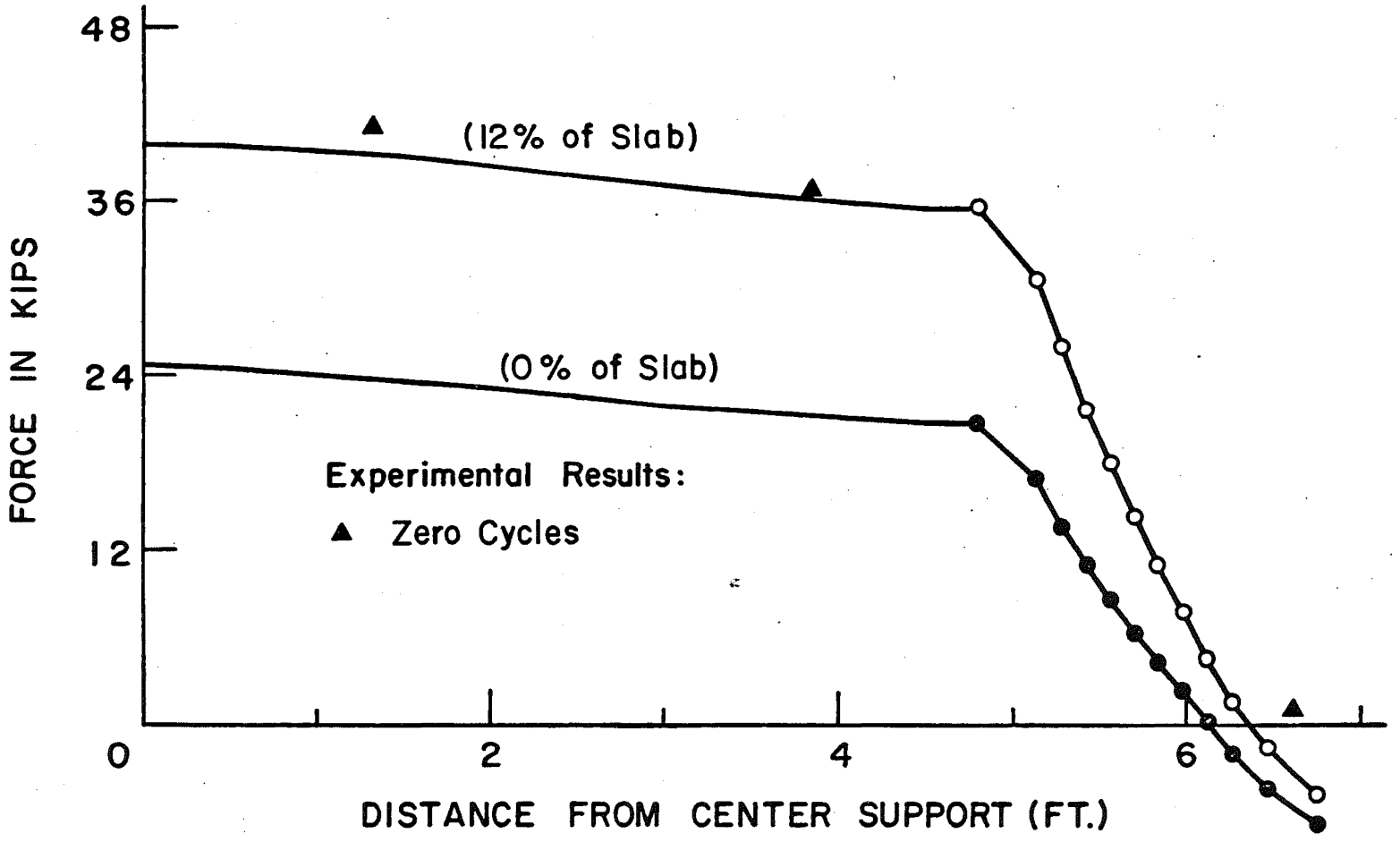

Fig. 21 Slab Force Curve for Beam CC-3F

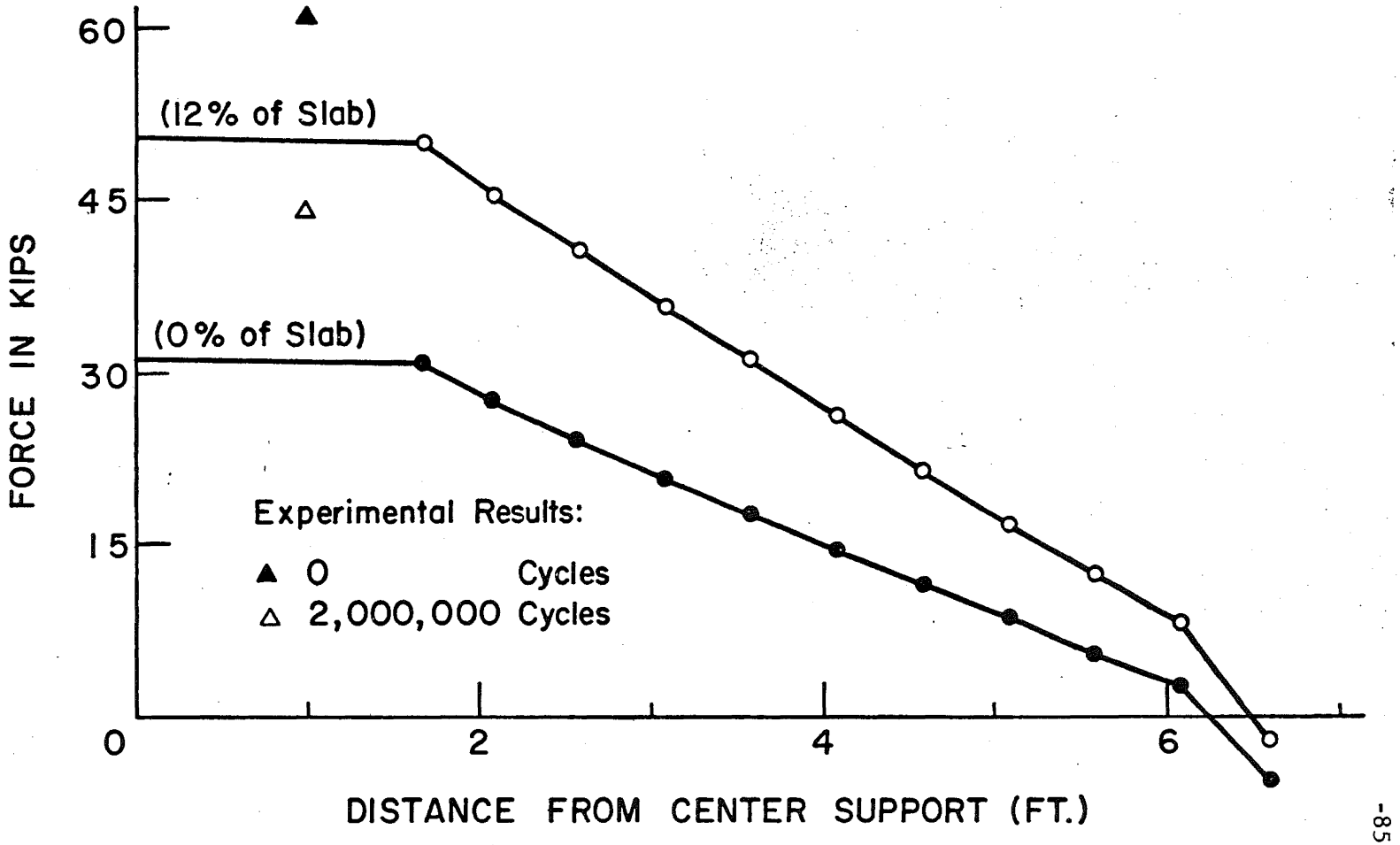

Fig. 22 Slab Force Curve for Beam CC-2F

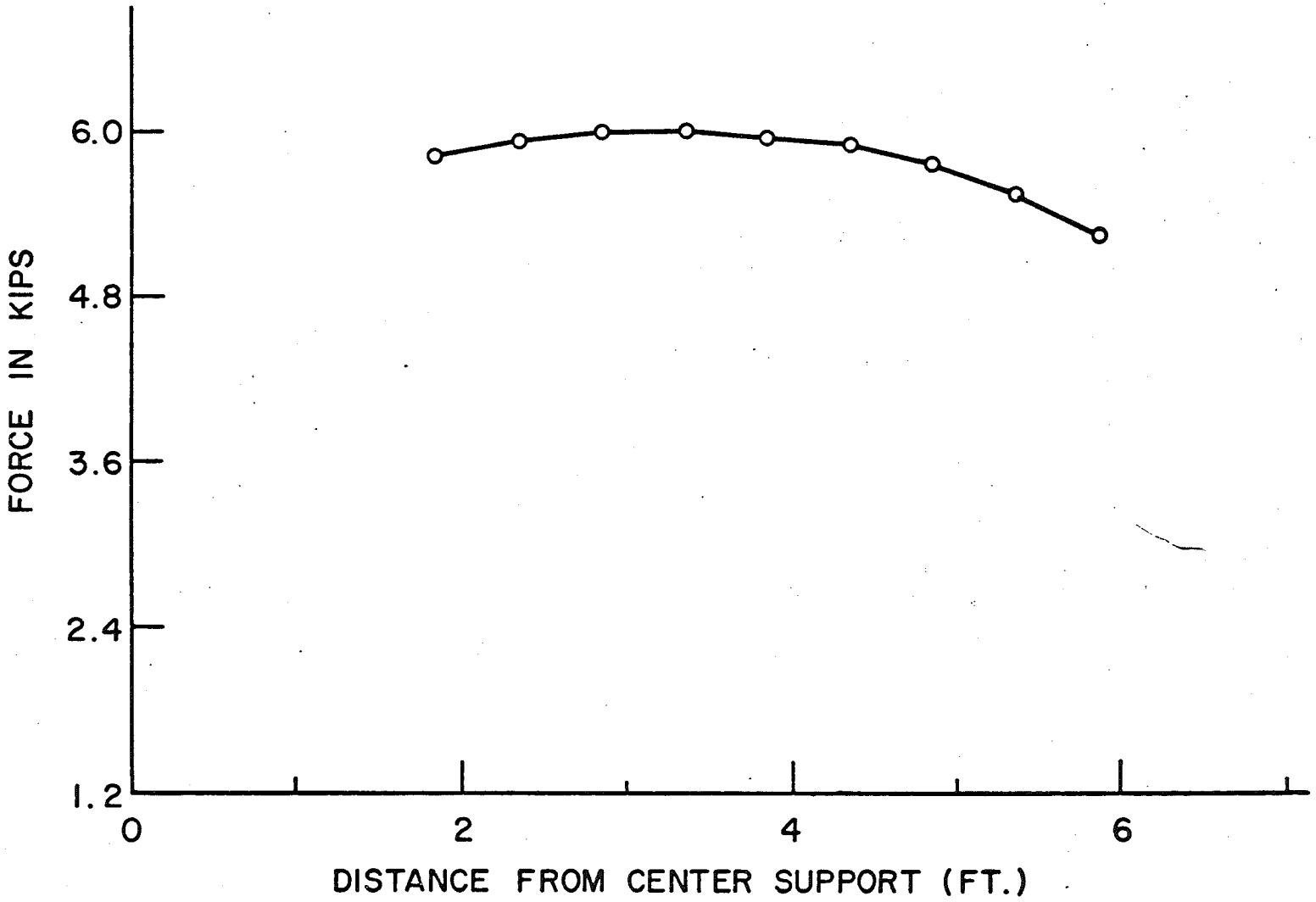

Fig. 23 Connector Force Curve for Beam CC-2F

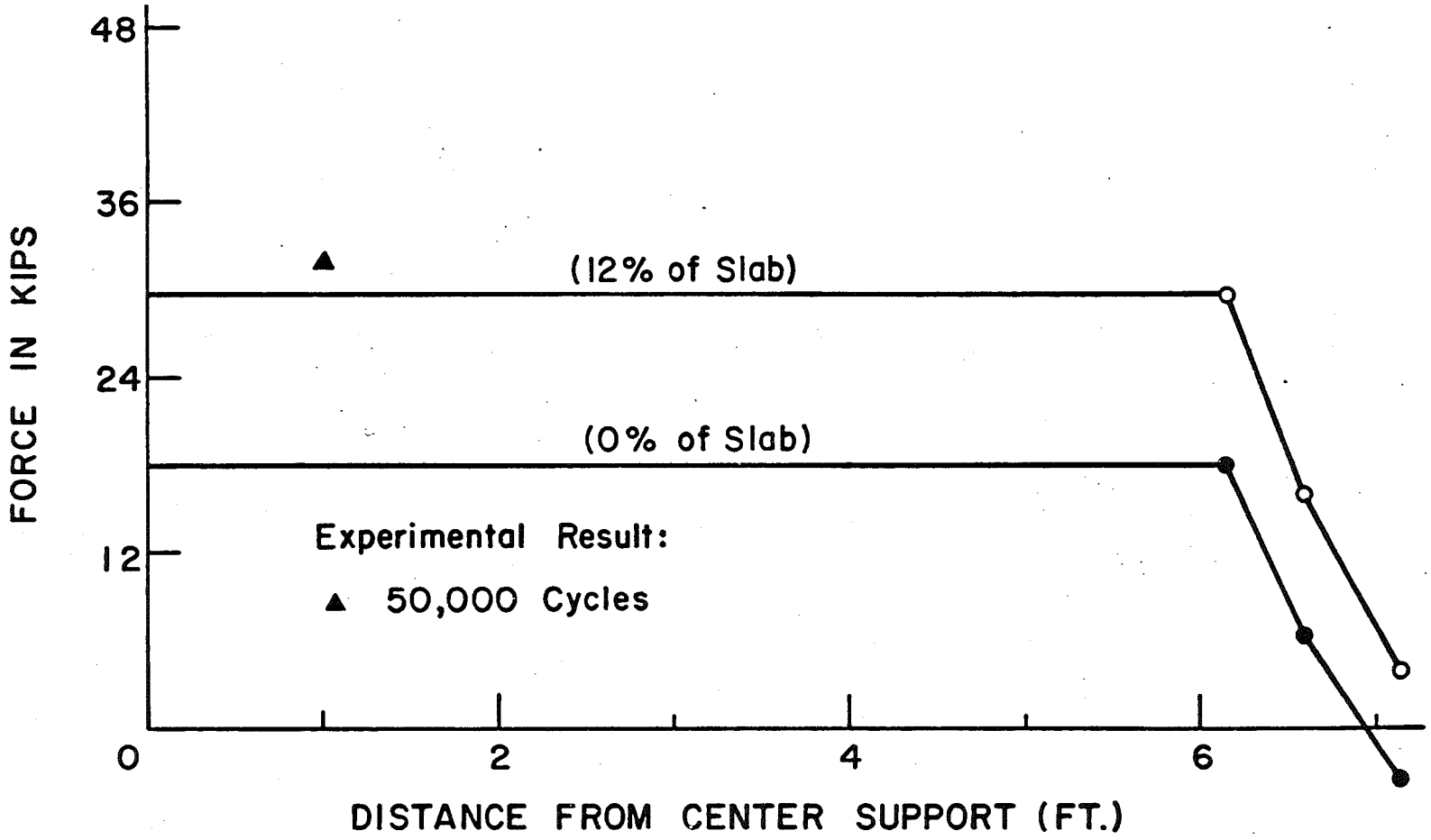

Fig. 24 Slab Force Curve for Beam CC-1F

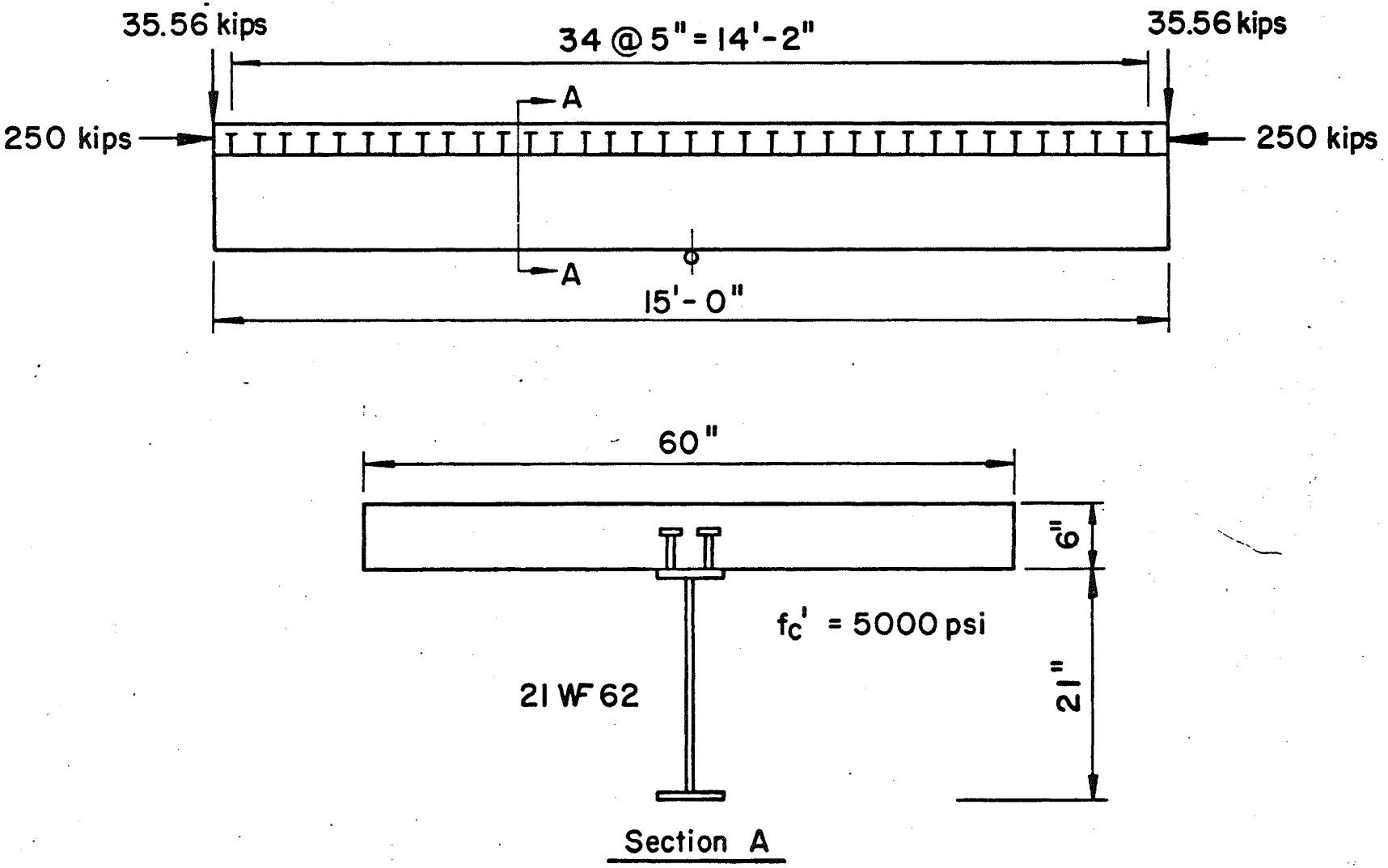

Fig. 25 Prestressed Composite Beam

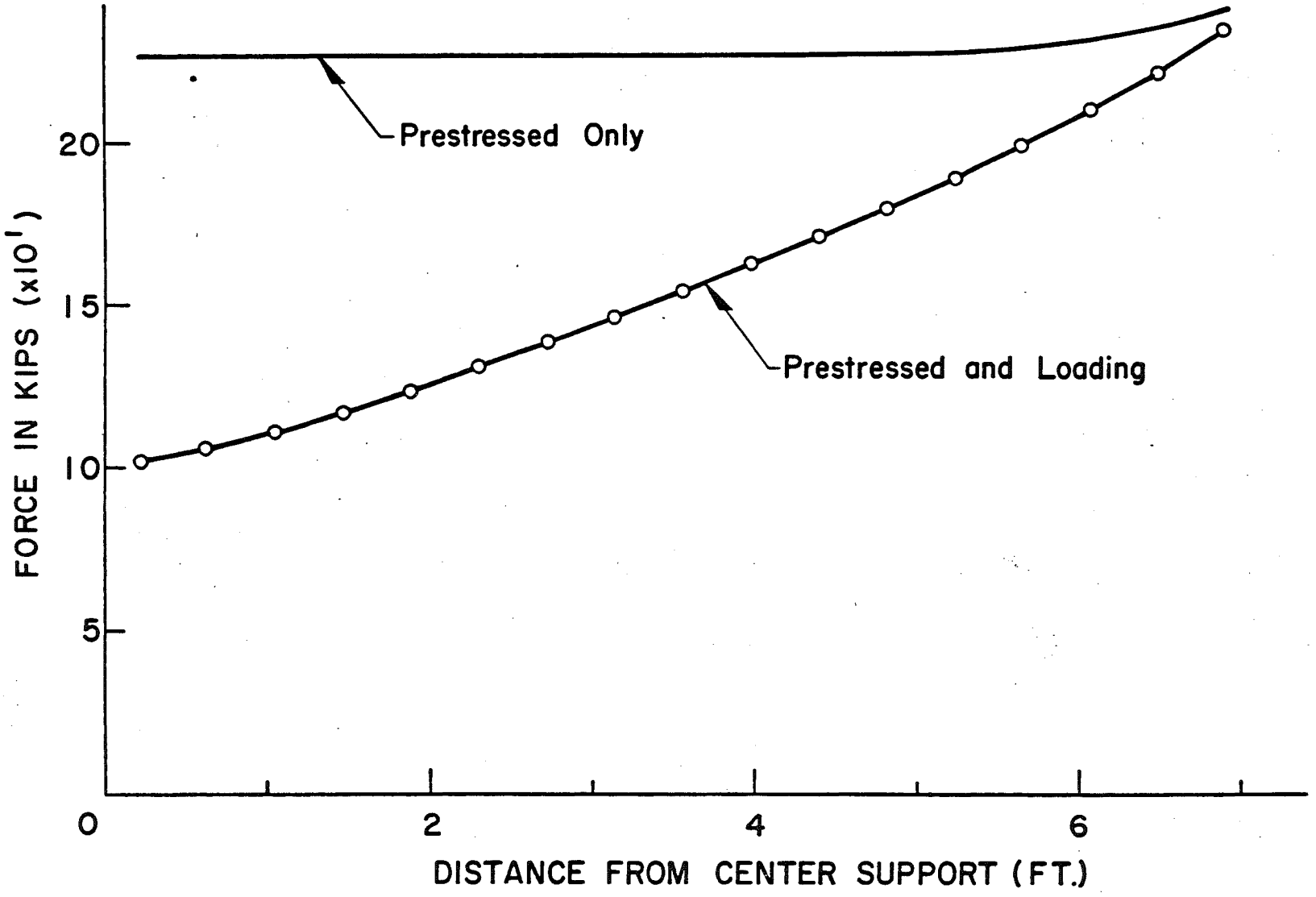

Fig. 26 Slab Force Curve for Prestressed Composite Beam

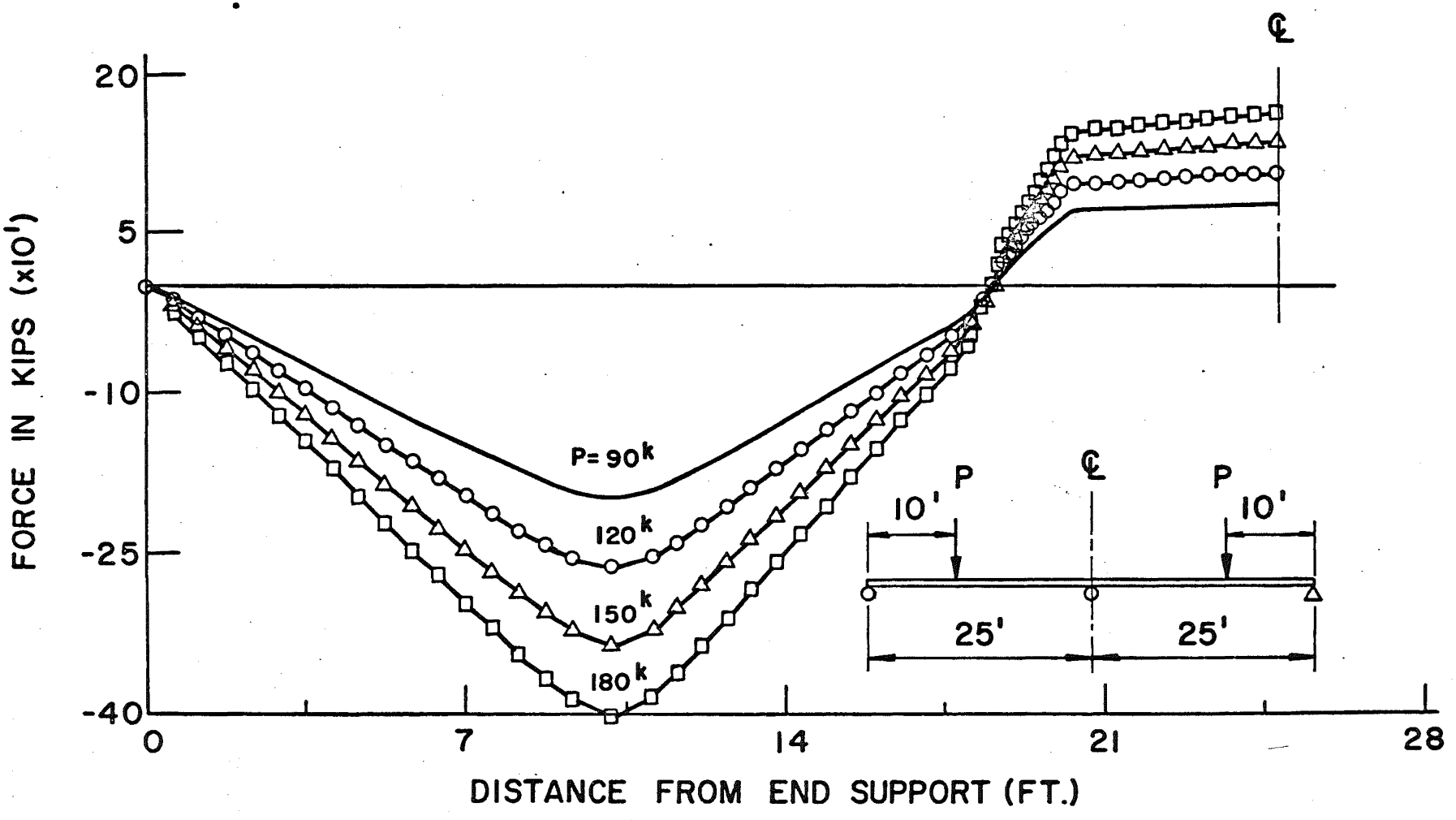

Fig. 27 Slab Force Curve for Beam CC-4F

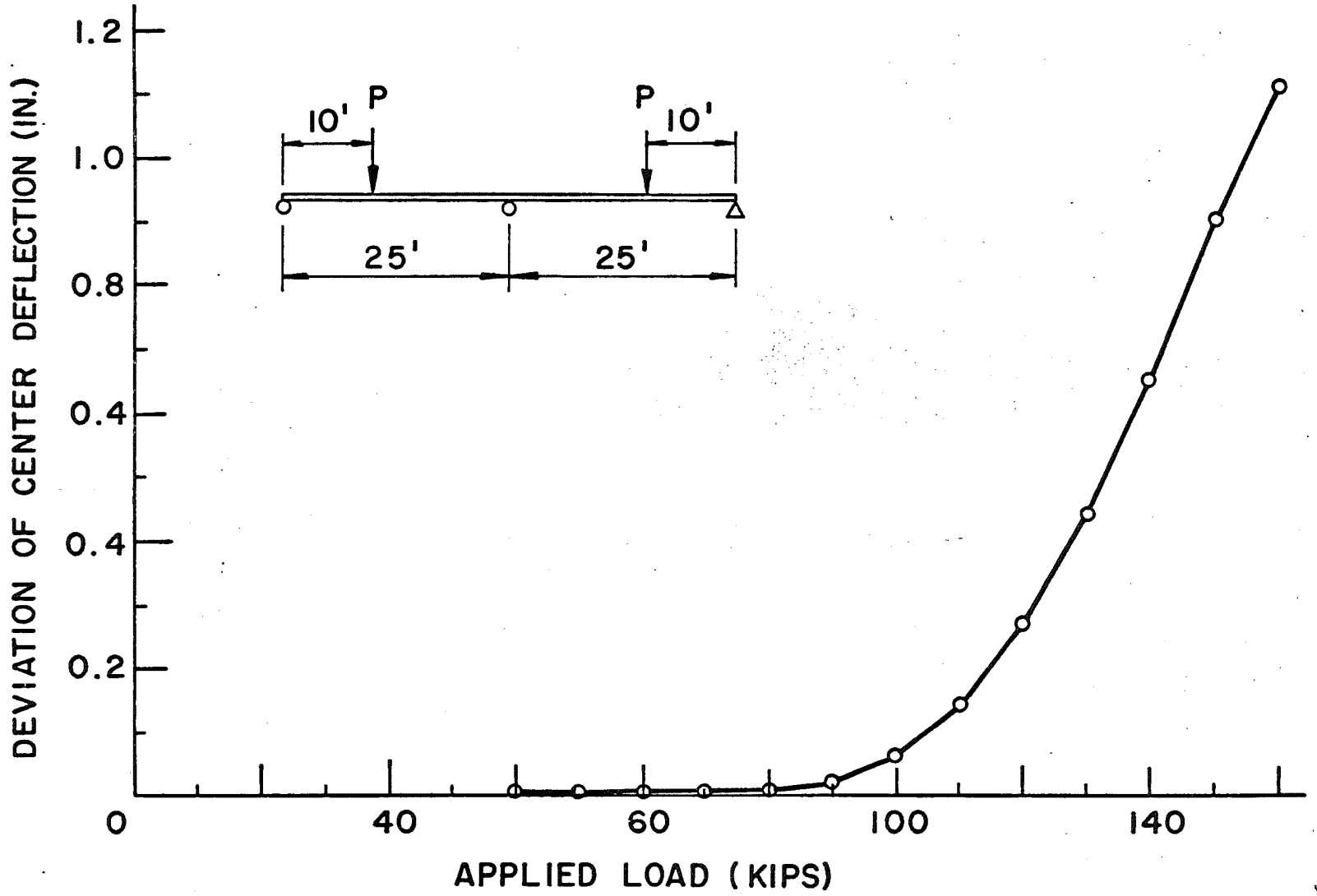

Fig. 28 Apparent Interior Support Settlement Produced by the Assumption of Fixed Points of Contraflexure

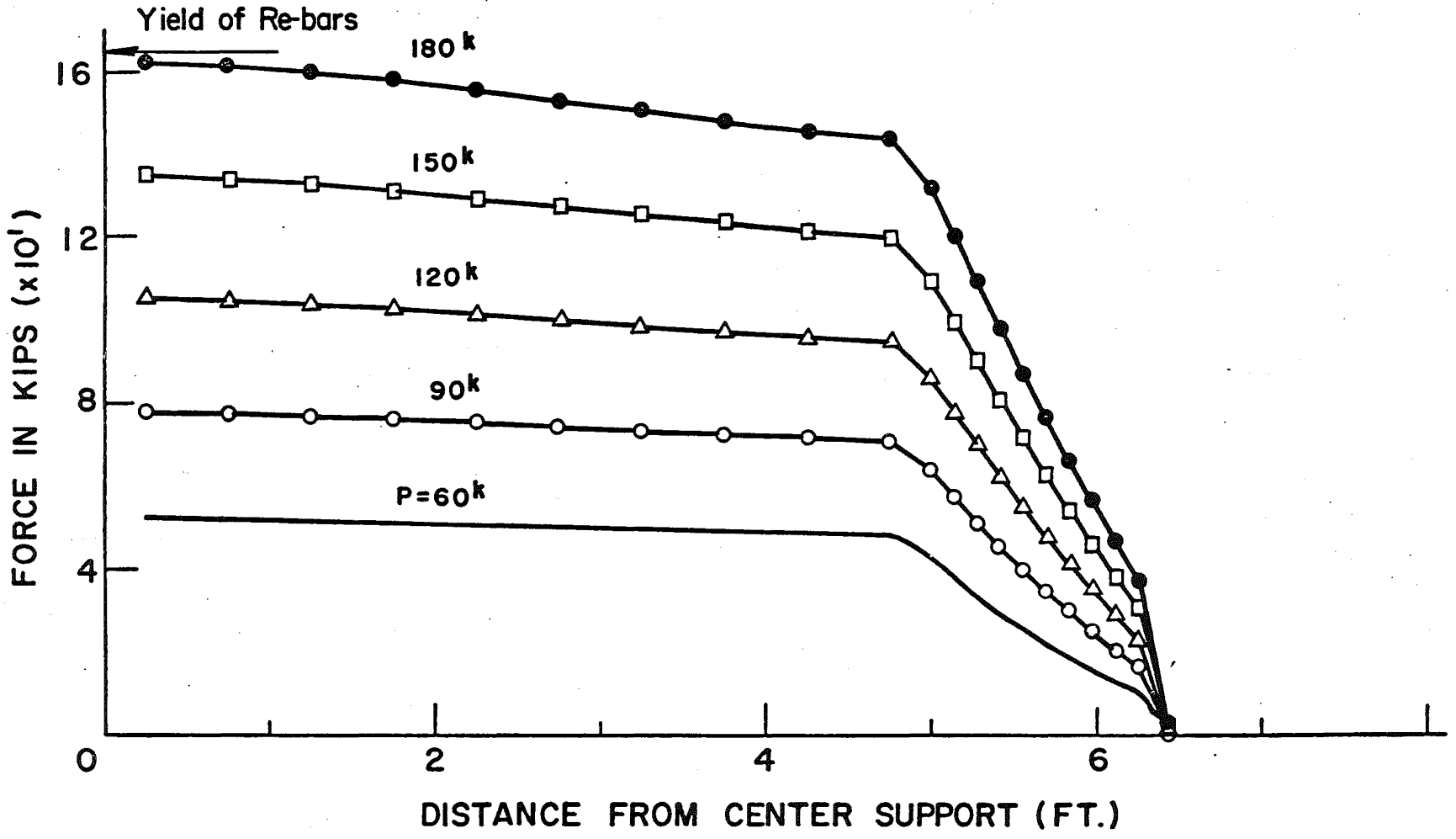

Fig. 29 Slab Force Curve for Beam CC-4F

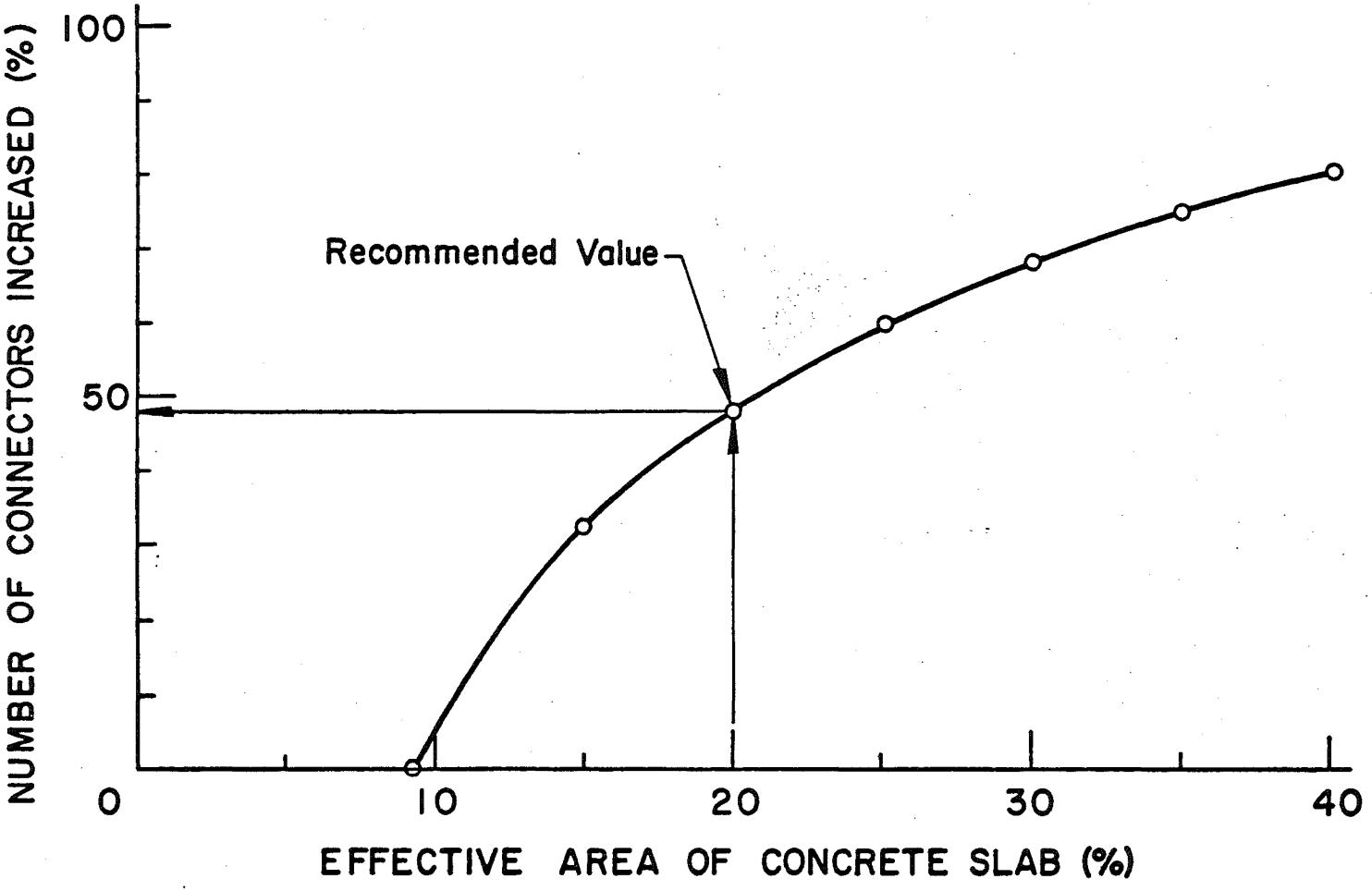

Fig. 30 Effect of Concrete Area on Connector Requirements

REFERENCES

1. Viest, Ivan M.
   REVIEW OF RESEARCH ON COMPOSITE STEEL CONCRETE BEAMS, Journal ASCE, Structural Division, Vol. 86, ST6, June 1960

2. AASHO
   STANDARD SPECIFICATIONS FOR HIGHWAY BRIDGES, Washington, D. C., 1944

3. AISC
   COMMENTARY ON PLASTIC DESIGN IN STEEL, Manual of Engineering Practice, No. 41, 1961

4. Johnson, R. P., Greenwood, R. D. and Dalen, K. V.
   STUD SHEAR CONNECTORS IN HOGGING MOMENT REGIONS OF COMPOSITE BEAMS, Structural Engineer, Vol. 47, No. 9, September 1969

5. AASHO
   STANDARD SPECIFICATIONS FOR HIGHWAY BRIDGES, Tenth Edition, American Association of State Highway Officials, 1969

6. AISC
   STEEL CONSTRUCTION MANUAL, Seventh Edition, New York, 1970

7. British Standards Institution
   COMPOSITE CONSTRUCTION IN STRUCTURAL STEEL AND CONCRETE BEAMS FOR BRIDGES, C.P. 117, Part 2, 1967

8. Stussi, F.
   ZUSAMMENGESETZTE VOLLWANDTRAGER, International Association of Bridge and Structural Engineering, Vol. VIII, pp. 249-269, 1947

9. Siess, C. P., Viest, I. M., and Newmakr, N. M.
   SMALL-SCALE TESTS OF SHEAR CONNECTORS AND COMPOSITE T-BEAMS, Bulletin No. 396, Experimental Station, University of Illinois, 1952

10. Baldwin, J. W., Henry, J. R. and Sweeney, C. M.
    STUDY OF COMPOSITE BRIDGE STRINGERS, Phase II, University of Missouri, May 1965

REFERENCES (continued)

11. Dai, P. K., Thiruvengadam, T. R. and Siess, C. P.
INELASTIC ANALYSIS OF COMPOSITE BEAMS,
Proceedings of Speciality Conference on Steel
Structures, ASCE, June 1970

12. Kaldjian, M. J.
COMPOSITE AND LAYERED BEAMS WITH NON-LINEAR CONNECTORS,
Proceedings of Speciality Conference on Steel Structures,
ASCE, June 1970

13. Driscoll, G. C. and Slutter, R. G.
RESEARCH ON COMPOSITE DESIGN AT LEHIGH UNIVERSITY,
Proceedings, National Engineering Conference, AISC,
May 1961

14. Woolley, W. R.
CONTINUOUSLY REINFORCED CONCRETE PAVEMENT WITHOUT
JOINTS, Proceedings, HRB, Vol. 27, pp. 28-33, 1947

15. Shieh, Ying-Jer
THE THEORETICAL ANALYSIS OF SPECIAL PROBLEMS ON THE
CONTINUOUSLY REINFORCED CONCRETE PAVEMENTS,
Fritz Engineering Laboratory Report, June 1958

16. Wu, Yao-Ching and Slutter, R. G.
CONTINUOUS COMPOSITE BEAMS UNDER FATIGUE LOADING,
Fritz Engineering Laboratory Report No. 359.2,
Lehigh University

17. Garcia, I. and Daniels, H. J.
TESTS OF COMPOSITE BEAMS UNDER NEGATIVE MOMENT,
Fritz Engineering Laboratory Report No. 359.1

18. Daniels, J. H. and J. W. Fisher
FATIGUE BEHAVIOR OF CONTINUOUS COMPOSITE BEAMS,
Highway Research Borad Publication No. 253,
Washington, D. C.

19. Barnard, P. R., Johnson, R. P. et al
DISCUSSION ON ULTIMATE STRENGTH OF COMPOSITE BEAMS,
The Institution of Civil Engineers, Great George St.
Westminster, London, S. W. 1